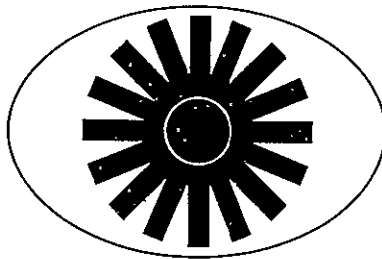


STRAIN RATE SENSITIVE CONSTITUTIVE EQUATIONS

TEES-9075-CR-71-001

by

CHARLES E. NELSON AND JAMES L. RAND



TEES

TEXAS ENGINEERING EXPERIMENT STATION  
TEXAS A & M UNIVERSITY  
COLLEGE STATION TEXAS 77843

August 1971

Prepared for  
NASA Manned Space Center  
Meteoroid Sciences  
Houston, Texas 77058

Under Contract NGR 44-001-106



FACILITY FORM 602

N71-38069  
(ACCESSION NUMBER)

93  
(PAGES)

CR-123175  
(NASA CR OR TMX OR AD NUMBER)

(THRU)

None  
(CODE)

17  
(CATEGORY)

STRAIN RATE SENSITIVE CONSTITUTIVE EQUATIONS

TEES-9075-CR-71-001

by

CHARLES E. NELSON AND JAMES L. RAND

August 1971

Prepared for

NASA Manned Spacecraft Center

Meteoroid Sciences

Houston, Texas 77058

Under Contract NGR 44-001-106

Prepared by

Texas Engineering Experiment Station

Texas A&M University

College Station, Texas 77843

#### FOREWARD

This report, TEES 9075-CR-71-001, is submitted by Texas Engineering Experiment Station in partial fulfillment of Contract NGR 44-001-106. It is also submitted by Charles E. Nelson to the Graduate College of Texas A&M University in partial fulfillment of the requirement for the degree of Master of Science in Aerospace Engineering in August 1971.

## ABSTRACT

Strain Rate Sensitive Constitutive Equations (August 1971)

Charles Edward Nelson, B.S., Texas A&M University;

Directed by: Dr. James L. Rand

The purpose of this research is to develop rate sensitive constitutive equations. The constitutive equations are analytic relations between stress and strain. The developed equations make use of a yield criterion which incorporates the second and third invariants of the stress deviator. The deviator defines a materials' change in shape. The resulting equation is applicable to any type of stress tensor. Values of stress and strain under uni-axial and torsional states of stress for various strain rates are generated. Stress-strain behavior at various strain rates is predicted for copper, lead, Al 1100 (99.00% pure), Al 1060-0 (99.60%), Annealed Aluminum (99.995%), and High Purity Al (99.997%). With the incorporation of rate sensitivity into the constitutive equations, a material's response to strain rates of  $10^6 \text{ sec}^{-1}$  and higher is predicted. A comparison is made between the response predicted by the constitutive equations and published experimental results. Good agreement exists at high strain rates, but as the dynamic strain rate approaches the "static" value small amounts of error are incurred.

## ACKNOWLEDGEMENT

The author wishes to express his sincere appreciation to Dr. James L. Rand for his interest and guidance throughout this research program. Special thanks are extended to Dr. U.S. Lindholm of the Southwest Research Institute with whose permission Figure 3 displaying "dynamic loading regimes" was reproduced. Appreciation is also given to Burton Cour-Palais of NASA-MSC and B. Chakrapani for their suggestions in the conduction of this research program. This research was supported under NASA Grant NGR 44-001-106.

## TABLE OF CONTENTS

	<u>Page</u>
ABSTRACT . . . . .	iii
ACKNOWLEDGEMENT . . . . .	iv
TABLE OF CONTENTS . . . . .	v
LIST OF TABLES . . . . .	vii
LIST OF FIGURES. . . . .	viii
NOMENCLATURE . . . . .	ix
CHAPTER	
I. INTRODUCTION . . . . .	1
The Need For a Strain Rate Sensitive Constitu-	
tive Equation . . . . .	1
Variations In Experimental Results . . . . .	2
Strain Rate Considerations . . . . .	3
II. LITERATURE REVIEW . . . . .	9
Experimental Investigation . . . . .	10
Theoretical Investigation . . . . .	16
III. DEVELOPMENT OF CONSTITUTIVE EQUATION. . . . .	26
General Discussion . . . . .	26
Formulation of Yield Criterion . . . . .	28
Incorporation of Yield Criterion . . . . .	31
Consideration of $\Phi$ Functions . . . . .	39
Induced Error . . . . .	46
Incorporation of $\Phi(F)$ Into the Constitutive	
Equations . . . . .	49

	<u>Page</u>
$\Phi(F)$ For Loadings Other Than Uni-Axial . . . . .	50
IV. RESULTS AND DISCUSSION . . . . .	56
Results and Concluding Remarks . . . . .	56
REFERENCES . . . . .	61
APPENDIX A DEVELOPMENT OF THE STRESS DEVIATOR . . . . .	64
APPENDIX B LEAST SQUARE FIT TO DATA . . . . .	68
APPENDIX C STRAIN RATE DATA . . . . .	73
VITA . . . . .	83

## LIST OF TABLES

	<u>Page</u>
Table 1 Computed Constants For Various Materials . . . .	47



## LIST OF FIGURES

	<u>Page</u>
Figure 1 Comparison of Rate Data For Commercially Pure Aluminum . . . . .	4
Figure 2 Dynamic Loading Regimes . . . . .	17
Figure 3 Yield Criteria . . . . .	32
Figure 4 Uni-axial Stress-Strain Rate Experiments On Annealed Aluminum . . . . .	44
Figure 5 Material Parameters For Annealed Aluminum, $\ln(e^F - 1) = M \ln(\dot{\epsilon} / \dot{\epsilon}_0) + C$ . . . . .	45
Figure 6 Stress-Strain Behavior In Shear For Aluminum 1100-0 . . . . .	55
Figure 7 Experimental and Theoretical Rate Sensitivity For Annealed Al (99.995% pure) . . . . .	74
Figure 8 Dynamic Response of Aluminum 1100-0 (Rand). .	76
Figure 9 Dynamic Response of Aluminum 1100-0 (Lindholm)	77
Figure 10 Dynamic Response of Annealed Aluminum (99.995% Pure) . . . . .	78
Figure 11 Dynamic Response of Copper . . . . .	79
Figure 12 Dynamic Response of High Purity Aluminum (99.997% Pure) . . . . .	80
Figure 13 Dynamic Response of Lead . . . . .	81
Figure 14 Dynamic Response of Aluminum 1060-0 . . . . .	82

## NOMENCLATURE

## Variable

$A_1, B_1, C_1$	= coefficient in expansion of slope by Eq. (61)
$A_2, B_2, C_2$	= coefficient in expansion of intercept by Eq. (61)
$C$	= intercept of $\ln - \ln$ plot in Fig. 4
$E$	= Modulus of Elasticity
$e_{ij}$	= component of the strain deviator
$\dot{e}_{ij}^{VP}$	= visco - plastic strain rate tensor
$F$	= static yield condition defined by Eq. (5)
$f$	= function relating second and third stress deviator defined by Eq. (28)
$G$	= Modulus of Rigidity
$J_1$	= first stress invariant
$J_2$	= second stress invariant
$J_3$	= third stress invariant
$J'_1$	= first invariant of the stress deviator
$J'_2$	= second invariant of the stress deviator
$J'_3$	= third invariant of the stress deviator
$k$	= constant in the yield condition
$L$	= elastic constant
$M$	= slope of $\ln - \ln$ plot in Fig. 4
$p$	= hydrostatic pressure
$S_{ij}$	= component of stress deviator

## Variable

$Y$	= yield stress
$\alpha$	= summation index
$\gamma_{ij}$	= shear strain tensor
$\dot{\gamma}$	= shear strain rate
$\dot{\gamma}_0$	= static shear strain rate
$\gamma^0$	= physical constant
$\epsilon_{ij}$	= strain tensor
$\epsilon''$	= plastic strain
$\dot{\epsilon}_0$	= static strain rate
$\dot{\epsilon}_{ij}^p$	= plastic strain rate tensor
$\dot{\epsilon}$	= strain rate for uni-axial loading
$\dot{\epsilon}''$	= plastic strain rate
$\mu$	= elastic constant
$\eta$	= coefficient of viscosity
$\nu$	= Poissons ratio
$\sigma_{ij}$	= stress tensor
$\sigma_0$	= static yield stress in pure shear
$\sigma_x$	= uni-axial stress
$\sigma$	= dynamic uni-axial stress
$\tau_{ij}$	= shear stress tensor
$\Phi(F)$	= rate sensitivity material parameter

## Subscript

uni-ax	= uni-axial loading
sh	= shear loading

## CHAPTER I

## INTRODUCTION

## 1.1 The Need For A Strain Rate Sensitive Constitutive Equation

Material response to various rates of deformation has long been of interest to scientists and engineers. The simulation of relatively low rates of strain can be obtained in the laboratory and until only recently, there has been no need to extend the testing ability to rates much greater than  $10^4 \text{ sec}^{-1}$ . Then, with the advent of the space age, engineers became interested in areas of high velocity impact and high rates of strain. Questions were asked as to how would a material respond when impacted by a particle traveling at 72.0 km/sec. Numerical simulations<sup>1,2,3</sup> were developed which attempted to predict the effects of these high speed events. But to adequately predict these effects, it became evident that some mathematical model needed to be developed which would describe the response of a material for different rates of loading.

From these early codes, predicting crater size for various size projectiles and impact velocities demonstrated the complex mechanism operative during a hypervelocity impact. The qualitative results which these investigators obtained were used to

---

The citations on the following pages follow the style of the AIAA Journal.

develop an understanding of the role played by material response in regions of high velocity impact. However, to gain a quantitative answer to high speed impact, material parameters such as strength and rate sensitivity were needed for inclusion in the numerical codes. This rate sensitivity, or time dependent behavior, along with a constitutive equation describing stress as a function of strain helped extend the understanding of high velocity impact. High velocity impact is normally characterized by a hydrodynamic state where shear effects are negligible. However, when the initial stages of hypervelocity impact have passed, strength effects of the impacted material must be considered in order to adequately describe the material's response. It is in these later stages of high velocity impact that rate sensitive equations are needed. A constitutive equation which is strain rate sensitive should be able to describe both the elastic and plastic response of a material and be capable of a smooth transition between the two regions. It should be capable of showing an effective change in the yield stress if the material is rate sensitive and conversely, no change if the material's response is rate insensitive.

## 1.2 Variations In Experimental Results

Even with the advent of devices to measure the rate sensitivity of a material, the conclusions from these experiments show a variation in effective strength for apparently the same material.

Lindholm<sup>4</sup> and Rand<sup>5</sup> both considered the dynamic loading of commercially pure aluminum for strain rates up to about  $10^3 \text{ sec}^{-1}$ . From these two studies it can be seen that for similar strains and strain rates, different stresses were encountered. See Fig. 1.

As can be seen from the data collected by these two investigators, even a slight variation in types of testing, residual stresses, and grain structure of samples can be enough of a difference to cause a change in the stress-strain curves. By comparing published strain rates for similar metals and alloys, it appears that no two results have the exact same stress-strain curve. In fact even the quasi-static data varies; some investigators<sup>5</sup> consider quasi-static to mean a strain rate of  $10^{-2} \text{ sec}^{-1}$  while others<sup>6</sup> consider a strain rate of  $10 \text{ sec}^{-1}$ .

Changing the temperature of a material will also affect the results of dynamic testing. The inclusion of thermal effects into a materials behavior will effect the constitutive results. For an increase in temperature, the effective strength decreases, which might be analogous to lowering the rate of loading.

### 1.3. Strain Rate Considerations

The constitutive equations developed by Perzyna<sup>7</sup> are for generalized states of stress. He developed a general three dimensional elastic - viscoplastic model for rate sensitive materials and it is his work that is extended by this research. By using his generalization of the constitutive equation

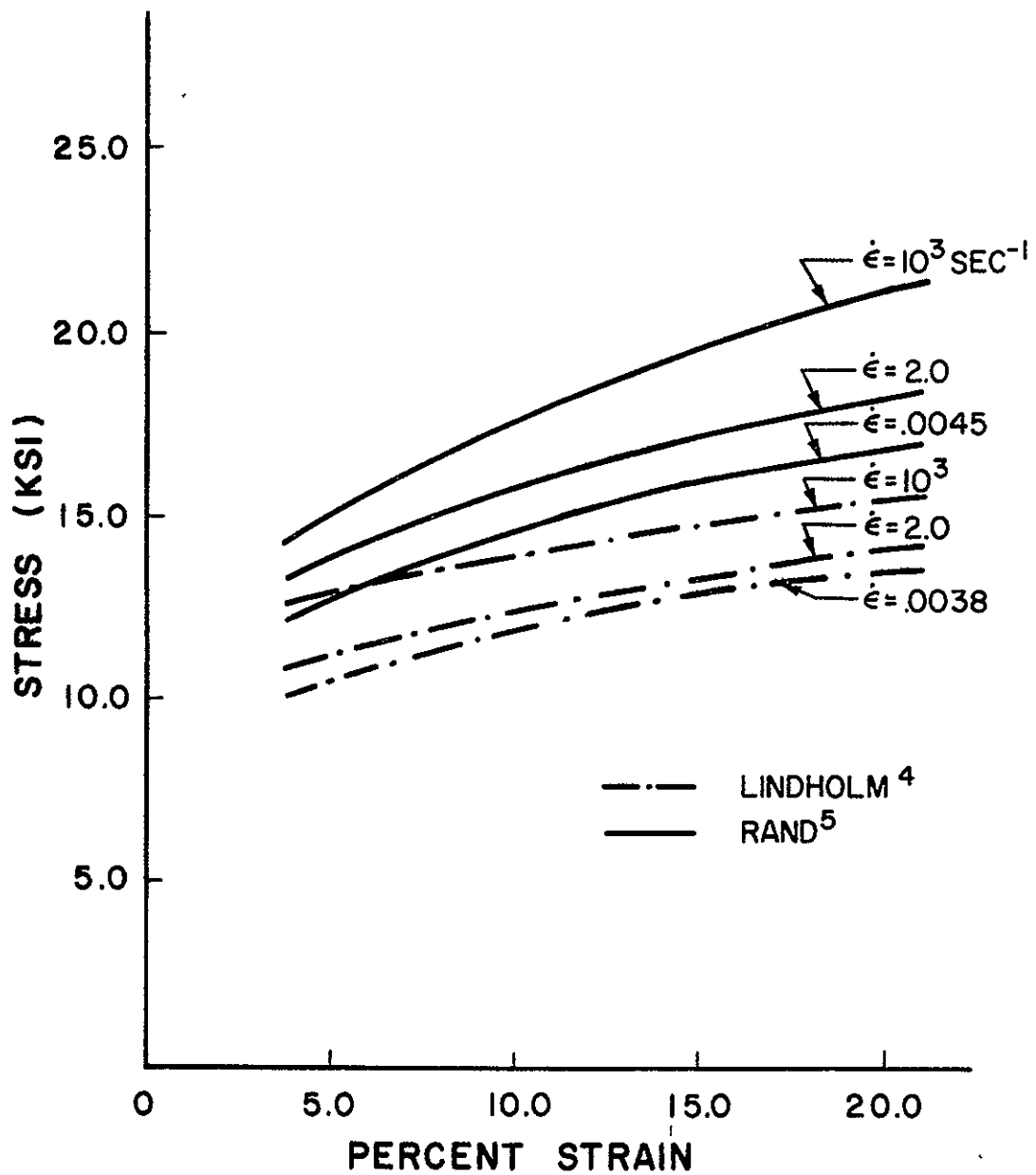


FIGURE 1 - COMPARISON OF RATE DATA FOR  
COMMERCIALLY PURE ALUMINUM

$$\begin{aligned}
\dot{\epsilon}_{ij} &= \frac{1}{2\mu} \dot{S}_{ij} + \gamma^0 \Phi(F) \frac{\partial F}{\partial \sigma_{ij}} & \text{for } F > 0 \\
\dot{\epsilon}_{ij} &= \frac{1}{2\mu} \dot{S}_{ij} & \text{for } F \leq 0 \\
\dot{\epsilon}_{ii} &= \frac{1}{3L} \dot{\sigma}_{ii}
\end{aligned} \tag{1}$$

where

$S_{ij}$  = component of stress deviator

$e_{ij}$  = component of strain deviator

$\epsilon_{ii}$  = strain tensor

$\mu, L$  = elastic constants

$\sigma_{ij}$  = stress tensor

$\dot{\phantom{x}}$  = total time derivative

$\gamma^0$  = physical constant

$\Phi(F)$  = results of material behavior under dynamic loading.

Any function,  $F$ , which represents the static yield condition will satisfy the above equation. That is

$$F = \frac{f(J'_2, J'_3)}{\sigma_0} - 1 \quad \text{if } f(J'_2, J'_3) > \sigma_0$$

where  $J'_2$  and  $J'_3$  are the second and third stress invariants of the stress deviator which are developed in Appendix A. The expression  $\sigma_0$  is the yield stress.



By considering the non-elastic part of the strain rate tensor, we get

$$\dot{\epsilon}_{ij}^p = \gamma^0 \phi(F) \frac{\partial F}{\partial \sigma_{ij}}, \quad (2)$$

which means that for a plastic strain rate, some function  $\phi(F)$  may be chosen to represent the results of tests on the behavior of metals under dynamic loading. Once this function has been determined, the problem of investigating rate sensitive constitutive equations and describing a materials response is complete.

Various forms of this function  $\phi(F)$  have been suggested,<sup>7</sup> however after applying strain rate data<sup>1</sup> to the suggested forms, no apparent continuity existed and a new  $\phi(F)$  was developed. This new function is sensitive to strain rate data for the determination of material constants as will be seen for the two different sets of data on 1100-0 Aluminum. Determination of these material constants, requires having a prior knowledge of strain rate history, however by using data in the realm<sup>1</sup> of  $10^3 \text{ sec}^{-1}$ , predicting effective strengths for strain rates of  $10^6 \text{ sec}^{-1}$  becomes possible.

The forms of the function suggested by Perzyna<sup>7</sup> were either an exponential series

$$\phi_1(F) = \sum_{\alpha=1}^N A_{\alpha} [\exp(F)^{\alpha} - 1] \quad (3)$$

or a series expansion

$$\Phi_2(F) = \sum_{\alpha=1}^N B_{\alpha} F^{\alpha} \quad (4)$$

where  $F$  is the static yield function given by

$$F = \frac{J_2^{1/2}}{\sigma_0} - 1 = \frac{\{S_{ij} S_{ij} / 2\}^{1/2}}{\sigma_0} - 1 \quad (5)$$

For the uni-axial loading considered in this investigation,  $\sigma_x = \sigma$ , and  $\sigma_y = \sigma_z = 0$ , whereby  $F$  takes the form

$$F = \frac{\sigma}{\sigma_0} - 1 \quad (6)$$

By considering the form of  $\Phi(F)$  suggested, and with the comparison of strain rate data for Al 1100-0 (99.00% pure), Al 1060-0 (99.60%), Annealed Al (99.995%), High Purity Al (99.997%), copper, and lead it became apparent neither of these forms would adequately describe the material response. The evaluation of these functions will be discussed in greater detail in Chapter III along with the evaluation of a new expression for  $\Phi(F)$ .

In Chapter II past work in the area of rate sensitivity is reviewed. The review is broken down into two sections, theoretical wave propagation relating to strain rate and experimental investigations. In the theoretical section, discrepancies arise between the mathematical models due to the assumptions used to describe various material's response. For the experimental investigation,

rate sensitivity varied for a particular material among the investigators. The results and conclusions were in general consistent when the entire area of dynamic material response was considered.

Chapter III considers the form of the rate sensitive constitutive equation developed and explains how the equation predicts various stress-strain curves for various strain rates. The amount of error incurred by using this form of equation is discussed and a comparison of predicted values with experimental results is shown.

In Chapter IV, the results and conclusions are made concerning the rate sensitive equation along with further possibilities concerning a better refinement of the  $\Phi(F)$  function. Also discussed is the applicability of this equation to torsional loading situations. Discussion is also directed toward the materials' effective yield strength at high rates of strain encountered during a hypervelocity impact. The application of a rate sensitive constitutive equation to high velocity impact compliments the hydrodynamic models initially considered for these problems which were insensitive to strength.

## CHAPTER II

### LITERATURE REVIEW

Recently the question of strain rate effects seem to be playing a more important part in dynamic testing of materials than it has in the past. It has been concluded that during dynamic testing, materials behave differently than when tested statically. Many theoretical and experimental studies have been devoted to observing this effect. Various effects have been observed, but it is rather difficult to describe them mathematically, and therefore give a full description of a material's response to different rates of loading. The magnitude of the rate of strain at which a particular material begins to be rate sensitive varies from material to material. Cristescu<sup>8</sup> feels the limiting rate of strain for some materials can be as low as  $10^{-4}$  sec<sup>-1</sup>.

To understand strain rate problems, an investigation of theoretical and experimental work should be considered. Some experimental investigators disregarded wave propagation phenomena although the rate of loadings are high. There are cases where stresses and strains are averaged out and the result can be indicative of the dynamic properties of the materials considered. This averaging of the stress and strain can only be considered if the specimen is small compared to the length of the loading pulse. However, conclusions in this area are sufficiently inconsistent to warrant further investigation into the rate influence of certain materials.

In the present study, rate effects of materials are broken down into two sections. The first being that of experimental results, in which the constitutive relations are determined for various rates of loading and secondly, a theoretical investigation which describes adequately a general constitutive equation for a particular material.

From a theoretical standpoint, an ideal rate sensitive constitutive equation should be capable of describing the various aspects of mechanical behavior normally encountered during any rate of loading. This equation should be capable of describing both the elastic and plastic part of the stress-strain curve and also be capable of a smooth transition between these two regions of behavior. However, presently there seems to be no single constitutive equation which adequately describes all aspects of mechanical behavior.

## 2.1. Experimental Investigation

Probably the first experiments dealing with strain rate sensitivity were conducted by B. Hopkinson<sup>9</sup> who studied the propagation of longitudinal waves in wire. He observed that the dynamic yield stress was approximately twice that of the static yield stress. After this initial work by Hopkinson, the study of rate sensitivity received little attention until Taylor and Quinney<sup>10</sup> did experimental work on mild steel and copper. In their investigation, they showed that due to the dynamic loadings, the dynamic yield

for steel was much larger than that in the static case, and for copper it was only slightly higher. Consequently, steel has more strain rate sensitivity than copper. Drucker<sup>11</sup> considered several classes of mathematical theories of plasticity for work-hardened materials and compared their advantages, disadvantages, and agreements with experiments. He even went so far as to make a distinction between various types of loadings and deformation in an attempt to explore and generalize the stress-strain relations.

Naghdi, et al.<sup>12</sup> did an experimental study of the initial and subsequent yield surface in plasticity. Their investigation concluded that 24ST-4 aluminum alloy subjected to torsion-tension reversed torsion produced an initial and two subsequent yield surfaces. That is, it showed three distinct stress-strain curves. Cook<sup>13</sup> did an extensive investigation on various steels for both a changing strain rate, and varying temperatures. He found that while yield stress generally increases with strain rate and decreases with temperature for any steel, the change in yield can be described by either a semi-logarithmic formula

$$\sigma = A \log \dot{\epsilon} + \sigma_0 \quad (7)$$

or a power law

$$\sigma = \sigma_0 B \dot{\epsilon}^\eta \quad (8)$$

where  $\sigma_0$  is the static yield,  $\dot{\epsilon}$  the strain rate,  $\sigma$  the dynamic yield, and A and B constants. In some cases, the first formula and in others the second adequately describe the experimental data, however, there did not seem to be any simple relationship. The same was also true for the temperature effects, no single formula covered all the data.

Kolsky and Douch<sup>14</sup> did an experimental study in plastic wave propagation. The measured dynamic stress-strain curves for specimens of pure copper, pure aluminum, and an aluminum alloy were generated by firing the specimens at a steel pressure bar. They found that for copper and aluminum the dynamic curves lay above the static ones, whereas for the aluminum alloy, there appeared to be no significant strain rate effect. Then with their dynamic results, they tried to test the prediction of a strain-rate independent theory by using plastic wave propagation. Bell,<sup>15</sup> who has done experimental work dealing with dynamic stress-strain curves, has concluded from experiments using diffraction-grating techniques that wave propagation is governed by strain rate independent theory and the static stress-strain curves.

Alter and Curtis<sup>16</sup> conducted tests to determine how pulses of plastic deformation disperse during propagation along a bar. It was shown in their study that wave dispersion cannot be due solely to the nonlinearity of a time independent stress-strain relation. However, a model not displaying rate parameters of a material exhibiting a strain rate sensitivity did not serve to adequately predict

the experimental observation. Thus they concluded that for lead the strain rate effect played an important part in controlling the behavior of a plastic strain pulse.

Lindholm and Yeakley,<sup>4</sup> in their experimental investigation of strain rate sensitive materials presented the split Hopkinson pressure bar method for obtaining complete stress-strain curves at high strain rates. Their strain rates were on the order  $10^3 \text{ sec}^{-1}$  in either tension or compression. Rand<sup>5</sup> also used the split Hopkinson pressure bar to determine the stress-strain curves for strain rates up to approximately  $10^3 \text{ sec}^{-1}$ . In his investigation, Rand analyzed in detail many of the assumptions and techniques used to obtain strain rate data. He also attempted to give an overall evaluation of the quality of the data generated by the pressure bar equipment based on one-dimensional wave analysis.

In the split Hopkinson pressure bar, the testing procedure consists of placing the specimen to be investigated between two pressure bars, both of which are cut from the same stock so as to have identical properties. An elastic driver bar is accelerated down the barrel of an air gun to impact one of the pressure bars. The stress waves caused by this impact travel down the elastic pressure bar until they reach the specimen. Then part of the stress waves are reflected and the remainder travel through the specimen into the last pressure bar. Strain gages on the pressure bars sense the stress waves and these stress waves are observed on an oscilloscope. By applying one dimensional wave



analysis to this recorded data, the velocity and force applied to the specimen can be determined. The stresses can then be found for any instant of time by averaging the forces and velocities.

Baron<sup>17</sup> considered rate sensitivity for metals and alloys at low temperatures. In his study, he varied the strain rates from about  $10^{-11}$  to  $10^4 \text{ sec}^{-1}$  and varied the temperature from  $20^\circ\text{C}$  to  $-196^\circ\text{C}$ . He noted that at these low strain rates, creep effects started to become effective, while at the high strain rates, wave propagation and inertia effects appeared.

Chiddister and Malvern<sup>18</sup> did experimental work for rate sensitivity on aluminum at elevated temperatures. With the introduction of elevated temperatures into rate sensitivity, these investigators found that strain rate dependence could be fitted by either a power function (log-log plot) or by a semi-logarithmic plot and that rate sensitivity was found to increase with temperature.

McLellan<sup>19</sup> has shown how inelastic stress-strain behavior can describe strain rate sensitive materials other than 2024-T4 aluminum in compression. In his study, he found that stress and strain rates are proportional on a logarithmic basis; and of the materials he examined, it was found that the rate of plastic flow was insensitive to strain rate.

Green,<sup>20</sup> et al. did a comprehensive strain rate study for aluminum and aluminum alloys in which they observed that the greatest rate sensitivity was in high purity aluminum (99.9999% pure)

and decreased with increasing impurity content (1060-0 and 1100-0 aluminum). That is, 99.9999% pure aluminum is more rate sensitive than Al 1060-0 or 1100-0, while Al 6061-T6 and Al7075-T6 are not rate sensitive at all. They theorized that impurities form stronger barriers to the motion of dislocations than the mechanisms predominant in high purity materials.

Karnes and Ripperger<sup>21</sup> did experimentation on specimens of high-purity polycrystalline aluminum to determine the amount of strain rate sensitivity. Their specimens were cold worked to varying degrees from an annealed condition to an engineering strain of 50%. They found, contrary to the prediction of the intersection mechanism of dislocation theory, that the cold working had little or no effect of the type or degree of strain rate sensitivity and that the material used in this study was strain rate sensitive regardless of the degree of cold working.

Lindholm,<sup>22</sup> considered the deformation of aluminum at strain rates from  $10^{-3} \text{ sec}^{-1}$  to  $10^3 \text{ sec}^{-1}$  and temperatures from  $300^\circ\text{K}$  to  $700^\circ\text{K}$ . In his work he considered stress states which included tension, compression, torsion, and combined tension and torsion. From the results he found that his tests compared favorable with the thermally-activated dislocation model of deformation.

Brown<sup>23</sup> conducted stress tests on thin walled tubes of polycrystalline 2024-T81 aluminum at temperatures of  $150^\circ\text{C}$  and  $250^\circ\text{C}$ . For steady state creep strain rates, the aluminum exhibited a considerable dependence on load history. For a certain history, he

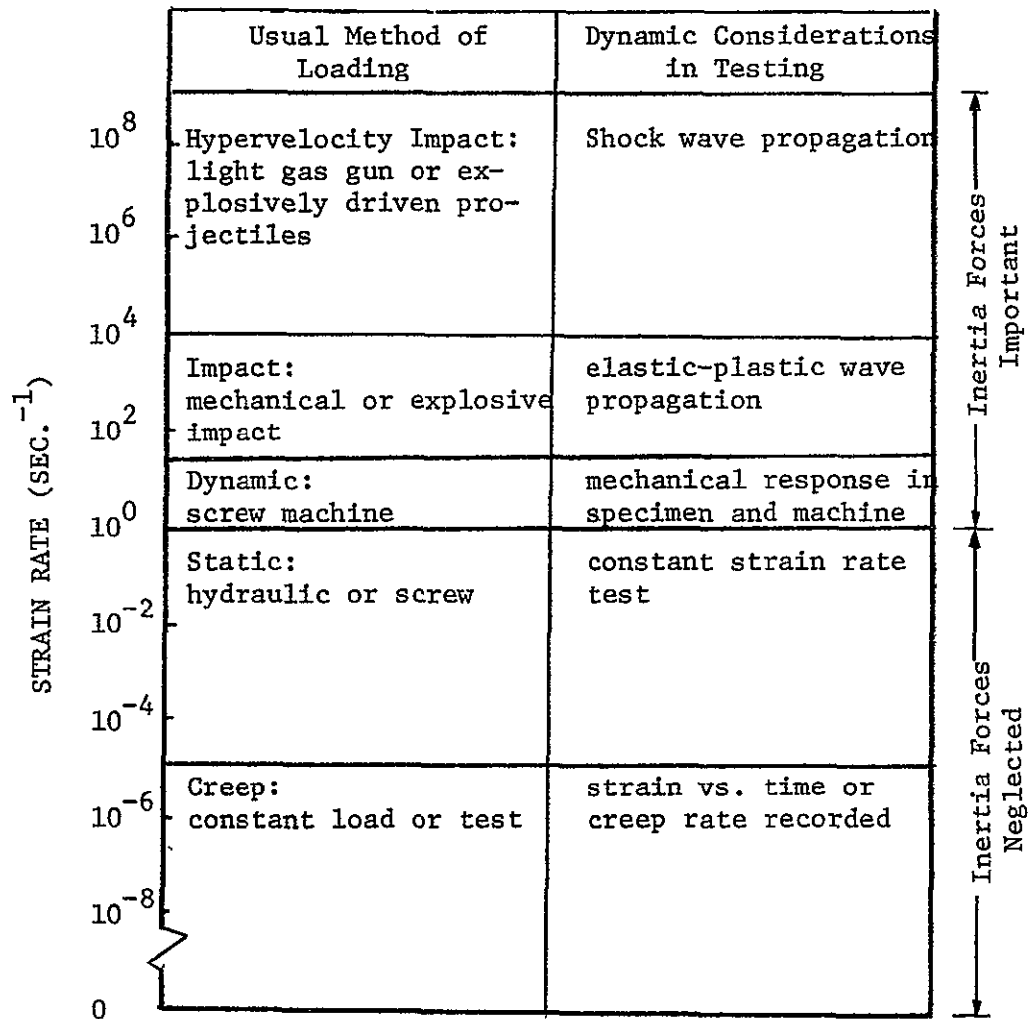
found it possible to determine unique surfaces of constant creep strain rate. In the temperature and small strain regions considered, room temperature yield surfaces were found to be unaffected by elevated temperature deformation.

Lindholm,<sup>24</sup> in his study of dynamic deformation of metals, has scaled strain rates from regions of creep to hypervelocity impact as can be seen in Fig. 2. Also included in his study of rate effects was a discussion of plastically deformed metals in terms of thermally activated dislocation mechanisms.

Bell<sup>25</sup> worked with "quasi-static," ( $10^{-2}$  to  $10^{-4}$  sec.<sup>-1</sup>) strain-rate data. He related the dynamic rate data to finite amplitude wave theory and includes a description of linear temperature-dependence. This theory is a generalized parabolic stress-strain law governing strain rate independent finite amplitude wave propagation in predicting dynamic and ultimate strength data.

## 2.2. Theoretical Investigation

To predict the performance of a structural system, it is necessary to consider the mechanical properties of the material. If the structure is subjected to strain rates greater than the static strain rate, then the resulting effect on the strength, modulus, and ductility of the material must be understood. An analytical description of the mechanical behavior by a constitutive equation which accounts for property changes with strain rate becomes necessary for accurate response calculations.

FIG. 2 Dynamic Loading Regimes<sup>24</sup>

Dynamic states of one-dimensional stress and one dimensional strain are usually the easiest to produce in the laboratory. While these are the easiest to investigate, they also represent the extreme bounds of an envelope of material behavior which includes most other states of stress.

In one dimensional stress, there is no restriction to lateral motion of the material. In one dimensional strain, the resistance is such that the lateral motion is nonexistent. Physically, this means that radial stress can be neglected and still obtain useful information.

Butcher and Karnes<sup>26</sup> present a discussion in which they use low strain rates as a starting point for their experimental analysis to understand strain rate sensitivity. In their theoretical investigation, they considered wave theory to calculate stress-strain curves for different strain rates. From their one dimensional loadings, and their wave analysis, they concluded that the stress-strain relations for a particular material determined under "quasi-static" conditions, may not be extended to dynamic conditions.

An effort to predict the propagation of plastic deformation was made during World War II, and then declassified in 1945. At this time, three investigators, von Karman of the United States, Taylor of England, and Rakhmatulin of the U.S.S.R. presented their theories on wave propagation. Rakhmatulin<sup>27</sup> studied the propagation of deformation along a bar due to a sudden pressure beyond the limit of elasticity and attempted to define a law of loading and

unloading. In his work, a process for the propagation of deformation was established. He started from the instant of time that deformation of an element occurs. The bar is loaded continuously up to a value predicted by  $\sigma = \sigma(\epsilon)$ , and then this deformation decreases depending on the form of load as well as the form of a new function,  $\sigma_1 = \sigma_1(\epsilon)$ . Also considered in this study was the form of the function  $\sigma = \sigma(\epsilon)$ , in which the scheme of Prandtl was examined. In this case, the distribution of residual deformation along the bar for an arbitrary change of load is considered.

About the time at which Rakhmatulin published his work, T. von Karman<sup>28</sup> of the United States investigated stress waves caused by longitudinal impact of a cylindrical bar. The bar was impacted with a velocity great enough to produce plastic strains. He presented a theory for computing the stress distribution along a bar at any instant after impact. He showed that for a given material there was a critical impact velocity, such that when subjected to a tension impact with a velocity larger than the critical velocity, the material would yield with small plastic strains.

Once the theory of plastic wave propagation was introduced, commonly referred to as the KTR theory, Malvern<sup>29</sup> developed a theory for longitudinal waves of plastic deformation. His development extended the KTR theory to include material properties in which the stress was a function of the instantaneous plastic strain and strain rate. He attempted to use solutions for idealized flow

laws where he compared his solution with those which neglected strain rate effects. He showed that for the existing theory of  $\sigma = \sigma(\epsilon)$ , considerable deviations were produced from the static stress-strain relations for changes in strain rate. He theorized that stress was a function of instantaneous plastic strain and strain rate. He assumed that there exists some relation where stress is defined as

$$\sigma = \sigma(\epsilon'', \dot{\epsilon}'') \quad (9)$$

and  $\epsilon''$  is the plastic strain and  $\dot{\epsilon}''$  the plastic strain rate.

Wood<sup>30</sup> presented a theoretical description which described the propagation of longitudinal plane waves of large lateral extent in solids for waves of plastic as well as elastic strain. He found that stress-strain characteristics of materials are, in general, dependent upon the duration and rates of loading, their wave propagation properties differing somewhat from those predicted from static stress-strain relations. He found that some materials were not affected much by a change in the impact loading and that the properties were confined primarily to the resistance of the materials to plastic shear strains. However, those materials that were affected by short loading times and high rates of deformation led to a change in the initial yield stress and a raising of the entire flow curve. Consequently, a change in the stress strain

curve due to impact loading was a direct result of the waves themselves.

However, the first theory which discussed the relationship of stress and strain rate was that presented by Hohenemser and Prager<sup>31</sup> in 1932. It was their work which attempted to define a possible rate sensitive constitutive equation. They theorized that the form of a constitutive equation could be defined as

$$2\eta \dot{\epsilon}_{ij}^p = 2\sigma_o \langle F \rangle \frac{\partial F}{\partial \sigma_{ij}} \quad (10)$$

where

$$F = \frac{J_2^{1/2}}{\sigma_o} - 1 = \frac{\{S_{ij} S_{ij} / 2\}^{1/2}}{\sigma_o} - 1 \quad (11)$$

is the static yield function and  $\epsilon_{ij}^p$  the components of the plastic or, more generally, the anelastic strain tensor,  $\eta$  is the coefficient of viscosity, and  $\sigma_o$  is the yield stress in simple shear. The stress deviator for uniaxial loading is nothing more than

$$\begin{bmatrix} \frac{2}{3}\sigma & 0 & 0 \\ 0 & -\frac{\sigma}{3} & 0 \\ 0 & 0 & -\frac{\sigma}{3} \end{bmatrix} = \begin{bmatrix} \sigma & 0 & 0 \\ 0 & 0 & 0 \\ 0 & 0 & 0 \end{bmatrix} - \begin{bmatrix} \frac{\sigma}{3} & 0 & 0 \\ 0 & \frac{\sigma}{3} & 0 \\ 0 & 0 & \frac{\sigma}{3} \end{bmatrix} \quad (12)$$

the difference between the stress tensor and the hydrostatic tensor.

The symbol  $\langle F \rangle$  is defined as



$$\langle F \rangle = \begin{cases} 0, F \leq 0 \\ F, F > 0 \end{cases} \quad (13)$$

For the elastic strains, Hohenemser and Prager took the elastic strains into consideration, and denoting by  $e_{ij}$  the components of the strain deviator and by  $\mu$  and  $L$  elastic constants, they obtained the relations

$$\begin{aligned} \dot{e}_{ij} &= \frac{1}{2\mu} \dot{s}_{ij} + \frac{1-\sigma_0 J_2'^{1/2}}{2\eta} s_{ij} \quad \text{if } J_2'^{1/2} > \sigma_0, \\ \dot{e}_{ij} &= \frac{1}{2\mu} \dot{s}_{ij} \quad \text{if } J_2'^{1/2} \leq \sigma_0, \\ \dot{e}_{ii} &= \frac{1}{3L} \dot{\sigma}_{ii} \end{aligned} \quad (14)$$

Thus, from the work of these two mathematicians, a constitutive equation for rate sensitive plastic materials was defined.

Following the work of Prager, Perzyna<sup>7</sup> generalized the one dimensional constitutive equations for rate sensitive plastic materials to general states of stress. He presented the dynamic yield condition for elastic, visco-plastic materials and also incorporated  $J_3$ , the third stress invariant, into his rate sensitive model.

Perzyna theorized that instead of using the term  $2 \sigma_0 \langle F \rangle$ , in equation (10) of the Hohenemser formula the expression  $\gamma^0 \Phi(F)$  could be used, where  $\gamma^0$  is a physical constant of the material, and where  $\Phi(F)$  satisfies the condition

$$\begin{aligned}\Phi(F) &= 0 & \text{if } F \leq 0 \\ \Phi(F) &\neq 0 & \text{if } F > 0\end{aligned}\tag{15}$$

Then when elastic strains are added, the constitutive equations take the form

$$\begin{aligned}\dot{\epsilon}_{ij} &= \frac{1}{2\mu} \dot{s}_{ij} + \gamma^0 \Phi(F) \frac{\partial F}{\partial \sigma_{ij}} & \text{for } F > 0 \\ \dot{\epsilon}_{ij} &= \frac{1}{2\mu} \dot{s}_{ij} & \text{for } F \leq 0 \\ \dot{\epsilon}_{ii} &= \frac{1}{3L} \dot{\sigma}_{ii}\end{aligned}\tag{16}$$

The term  $\Phi(F)$  is a function which is chosen to represent the results of the behavior of metals under dynamic loading. In his work, Perzyna felt that possible forms of the function  $\Phi(F)$  could be an exponential expression of  $F$ ,

$$\Phi = \sum_{\alpha=1}^N A_{\alpha} [\exp(F)^{\alpha} - 1]\tag{3}$$

or possibly a polynomial expansion

$$\Phi = \sum_{\alpha=1}^N B_{\alpha} F^{\alpha}\tag{4}$$

However he felt that for the determination of the expression

(3) and (4) the correlation of stress and strain for various strain rates must be studied extensively.

Rosenblatt<sup>32</sup> in an attempt to describe material response for hypervelocity impact attempted to incorporate Perzyna's expression for rate sensitive constitutive equations. Due to the fact that experimental strain rate data had not been generated for strain rates above  $10^4 \text{ sec.}^{-1}$ , and since hypervelocity impact (see Fig. 2) produces strain rates on the order of  $10^6 \text{ sec.}^{-1}$ , a strain rate sensitive constitutive equation is needed to predict material response for high strain rates. Consequently, in his study, Rosenblatt attempted to determine strain rate sensitive equations which would adequately describe the material response to high velocity impact. However, of the forms he considered, no single expression adequately predicted the material response for rates greater than  $10^6 \text{ sec.}^{-1}$ . Consequently to extend the  $\Phi(F)$  function he chose an additional equation, where by matching slopes and magnitude, he was able to predict rates greater than  $10^6 \text{ sec.}^{-1}$ .

Thus it can be concluded that during dynamic testing, materials behave differently than when tested statically. Many experimental and theoretical studies have been devoted to observing this effect. Various effects have been observed, but it is rather difficult to describe them mathematically, and therefore give a full description of a material's response to different rates of loadings. It is the purpose of this paper to develop a constitutive equation which incorporates rate sensitivity into the description of a material's

behavior at various rates of loading.

## CHAPTER III

## DEVELOPMENT OF CONSTITUTIVE EQUATIONS

## 3.1. General Discussion

It would be highly advantageous to have at one's disposal a general constitutive equation for a material which would be capable of describing in a single expression the various aspects of mechanical behavior normally encountered during the loading process. Such an equation should be capable of describing both the elastic and plastic response, and additionally, provide for a smooth transition between these two realms of behavior.

Presently there are two approaches considered in the formulation of constitutive equations for elastic-plastic bodies. The first is the rate theory based on the Prandtl-Reuss relation which considers intervals of plastic strain as proportional to the stress deviator. The second is the total strain theory based on the Hencky equations which consider plastic strain as proportional to the stress deviator. Although the theories differ in many areas, they both consider total deformation as consisting of a small recoverable elastic component and an irrecoverable plastic component.

Experiments have been conducted on a large number of materials to determine whether the rate theory or the total strain theory is more realistic. From the experimental results,<sup>17</sup> it appears that the rate theory follows more accurately the experimental results,

and it is this theory that is adapted for this work.

The rate theory of plasticity is essentially a dynamic theory<sup>7</sup>; the constitutive equations being formulated in terms of rates of stress and deformation. The description of purely elastic behavior in metals, given by Hooke's law for small strain, is not dynamic; it is based on a static strain rate state and a constrained initial configuration. However, as long as elastic strains remain small, a rate form of Hooke's law may be employed to describe elastic response. In fact, the elastic component of strain is described by the rate form of Hooke's law. Consequently, it becomes clear that the constitutive equations governing elastic-plastic response in metals are most naturally expressed in rate form.

For a large number of metallic solids, which exhibit little or no strain hardening, the classical elastic-linearly plastic body has proved to be a realistic model to describe material response. This classical response is characterized by two regions of mechanical behavior, each of which has its own constitutive equation. There is the elastic region in which Hooke's law applies and the plastic region where plastic flow equations are employed. In an effort to combine the constitutive equations of each region, a yield condition is applied.

Employing the elastic-linearly plastic model is not well suited to realistically describe the response of non-hardening materials for large deformations. In fact, when considering high impulse

loading in deformable bodies, the material response is normally characterized by shock waves, large deformations, and maximum states of stress exceeding that at which the material yields. In order to realistically describe the mechanical states experienced during high velocity loading, it becomes clear why a constitutive equation, more general than the one for a classical elastic-plastic, must be employed. A suitable model must be capable of accounting for non-linear effects arising from large distortions and finite compressions.

### 3.2. Formulation of Yield Criterion

It is obvious that the constitutive equations (16) are valid for any function  $F$  representing the static yield condition provided the assumptions concerning plastic material are satisfied, that is, that the function  $F$  does not depend on the strains. For instance, for

$$F = \frac{f(J_2', J_3')}{\sigma_0} \quad (17)$$

$\sigma_0$  is a quasi-static stress, the strain does not appear. Rosenblatt, in his analytical study of strain rate effects considered using only the  $J_2'$  component. However, most researchers feel that the third invariant has some influence on the yielding of materials.

Anticipating that the incorporation of the third invariant of the deviatoric stress tensor into the yield criterion of metals might give better strain rate sensitivity parameters and functions, the following type of relation was formulated. Ignoring the Bauschinger effect, it can be assumed that materials behave similarly in tension and compression. This points out that quadratic or even powers of stresses need to be considered. Therefore a  $\frac{2}{3}$  rd power is used for the third invariant as follows,

$$J_2' + k(J_3')^{\frac{2}{3}} = \frac{y^2}{3} + k\left(\frac{2y^3}{2}\right)^{\frac{2}{3}} \quad (18)$$

where  $k$  is a constant to be determined and  $y$  is the yield stress in tension.

To determine  $k$  and to see whether the slight deviation of the experimental points from the von Mises yield condition, which is

$$J_2' = \frac{y^2}{3} , \quad (19)$$

might be due to the influence of the third invariant, the classical experimental results of Taylor and Quinney<sup>10</sup> were used. Since they used thin walled tubes subjected to torque and axial loading, the above criterion simplified to a stress tensor.



$$\begin{bmatrix} \sigma_x & \tau_{xy} & 0 \\ \tau_{xy} & 0 & 0 \\ 0 & 0 & 0 \end{bmatrix} = \begin{bmatrix} \frac{2}{3} \sigma_x & \tau_{xy} & 0 \\ \tau_{xy} & -\frac{\sigma_x}{3} & 0 \\ 0 & 0 & -\frac{\sigma_x}{3} \end{bmatrix} + \begin{bmatrix} \frac{\sigma_x}{3} & 0 & 0 \\ 0 & \frac{\sigma_x}{3} & 0 \\ 0 & 0 & \frac{\sigma_x}{3} \end{bmatrix}$$

The first tensor on the right hand side of this equation is the deviatoric stress tensor. From this deviatoric stress tensor, where the prime denotes the deviator:

$$J'_1 = 0$$

$$J'_2 = \frac{\sigma_x^2}{3} + \tau_{xy}^2 \quad (20)$$

$$J'_3 = \frac{2}{27} \sigma_x^3 + \frac{1}{3} \sigma_x \tau_{xy}^2$$

Therefore, in order to satisfy the case of uniaxial stress, where

$$J'_2 + k(J'_3)^{2/3} = \frac{y^2}{3} + k\left(\frac{2}{27} y^3\right)^{2/3} \quad (21)$$

we get

$$\left(\frac{\sigma_x}{y}\right)^2 + 3 \left(\frac{\tau_{xy}}{y}\right)^2 + 3k \left\{ \frac{2}{27} \left(\frac{\sigma_x}{y}\right)^3 + \frac{1}{3} \left(\frac{\sigma_x}{y}\right) \left(\frac{\tau_{xy}}{y}\right)^2 \right\}^{2/3} = \quad (22)$$

$$1. + .529134k$$

This polynomial is solved using the computer to find  $\tau_{xy}/y$  for each experimental value of  $\sigma_x$  and different values of  $k$ . It was found that the preceding equation agrees well with the experimental results of Taylor and Quinney for aluminum, copper, and mild steel, and are plotted in Fig. 3. The value of  $k = 0.0$  corresponds to the Von Mises condition and  $k = -0.13$  corresponds to the inclusion of  $J'_3$ . Hence, for further study of yield criteria, the equation

$$J'_2 - 0.13 (J'_3) = \frac{y^2}{3} (1 + k^3 \sqrt{\frac{4}{3}}) \quad (23)$$

will be used to predict yielding for all other materials.

It is also concluded on the basis of the limited data available, that the effect of the third invariant is more pronounced at the combinations of lower normal stress and higher shear stresses. However, as to the exact significance of adding the third invariant to the yield criterion warrants further investigation.

### 3.3 Incorporation of Yield Criterion

On the basis of including both  $J'_2$  and  $J'_3$  in the yield criterion, the form of the static yield function,  $F$ , can now be established. In order to apply the conditions of uni-axial loading, the stress deviator is nothing more than equation (12).

So that:

$$J'_1 = 0$$

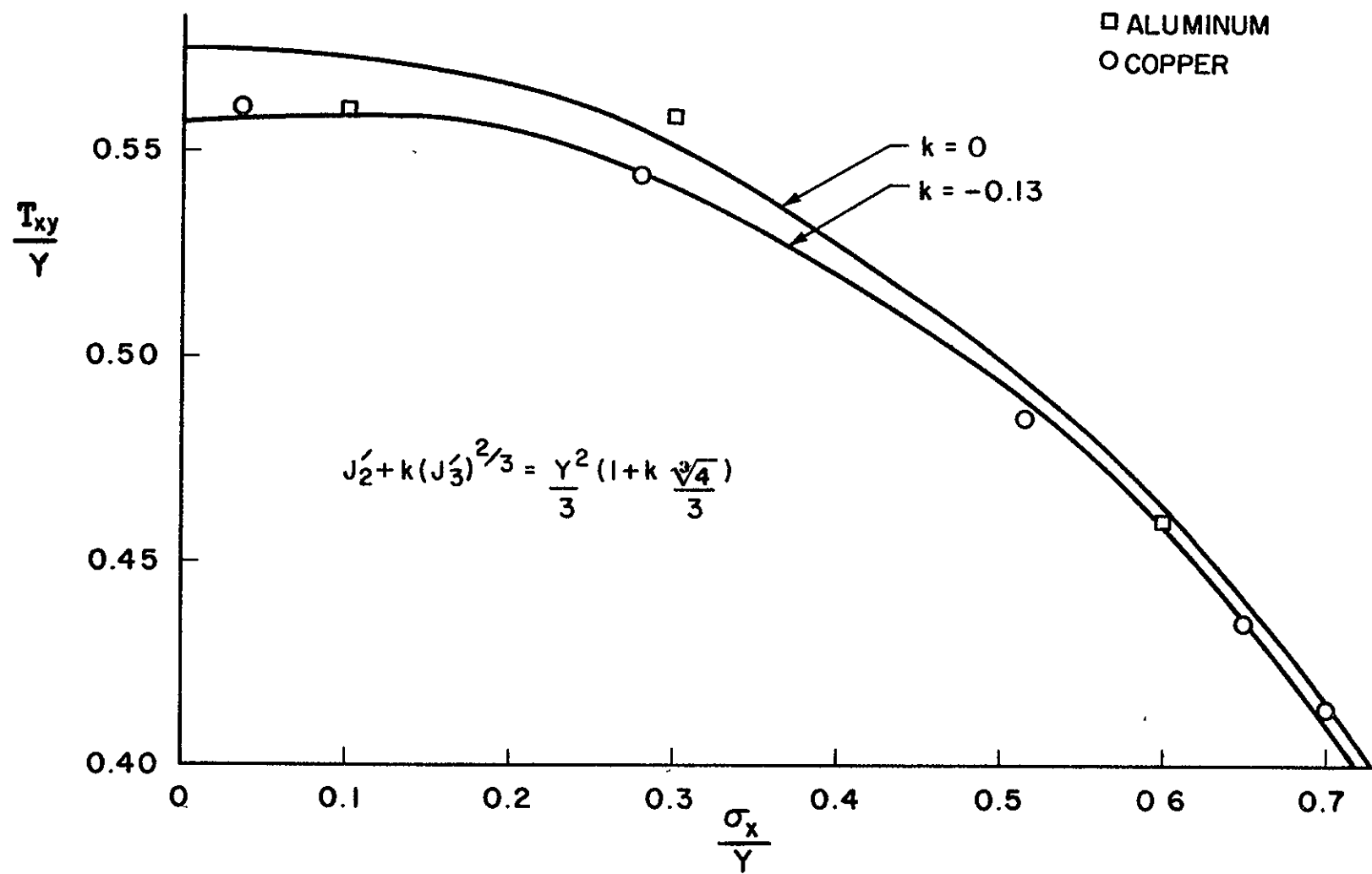


FIGURE 3 - YIELD CRITERIA

$$J_2' = \frac{\sigma^2}{3} \quad (24)$$

$$J_3' = \frac{2}{27} \sigma^3$$

From the prescribed definition of  $f$  used by Perzyna<sup>7</sup>

$$f = \sqrt{J_2'} \quad (25)$$

and defining  $\sigma_o$  as the yield stress in pure shear, the value of  $F$  becomes

$$F = \frac{(J_2')^{\frac{1}{2}}}{\sigma_o} - 1. \quad (26)$$

Now by applying the  $J_3'$  component and defining  $y$  as the yield stress in pure tension

$$F = \frac{f(J_2', J_3')}{y} - 1 \quad (27)$$

we have

$$f(J_2', J_3') = \left[ J_2' - 0.13(J_3')^{2/3} \right]^{1/2} \quad (28)$$

and

$$y = \left[ \frac{\sigma^2}{3} - 0.13 \frac{3\sqrt{4}}{9} \sigma_o^2 \right]^{1/2} \quad (29)$$

where

$$\sigma_o = (3)^{-1/2} y \quad (30)$$

the value of  $F$  becomes

$$F = \frac{\left[ J_2' - 0.13 (J_3')^{2/3} \right]^{1/2}}{\left[ \frac{\sigma_o}{3} - 0.13 \sqrt[3]{4} \sigma_o^2 \right]^{1/2}} - 1 \quad (31)$$

but for uni-axial loading,

$$J_2' = \frac{\sigma^2}{3} \quad (32)$$

$$J_3' = \frac{2}{27} \sigma^3$$

thus by substitution into (32),  $F$  becomes

$$F = \frac{\left[ \frac{\sigma^2}{3} - 0.13 \left( \frac{2}{27} \sigma^3 \right)^{2/3} \right]^{1/2}}{\left[ \frac{\sigma_o^2}{3} - 0.13 \frac{\sqrt[3]{4}}{9} \sigma_o^2 \right]^{1/2}} - 1$$

then by factoring and cancelling

$$F = \frac{\sigma}{\sigma_o} - 1 \quad (33)$$

With the form of  $F$  and  $f$  defined, it is now possible to consider the visco-plastic portion of the generalized constitutive equation.

That is

$$\dot{\epsilon}_{ij}^{vp} = \gamma \Phi(F) \frac{\partial F}{\partial \sigma_{ij}} \quad (34)$$

where  $\dot{\epsilon}_{ij}^{vp}$  is visco-plastic strain rate tensor,  $\gamma$  is a material

constant,  $\Phi(F)$  is a analytic solution relating stress, strain, and strain rate, and  $\sigma_{ij}$  is the stress tensor.

Considering the term  $f$ , defined by equation (28) the expression

$$\frac{\partial F}{\partial \sigma_{ij}} \text{ becomes } \frac{\partial F}{\partial \sigma_{ij}} = \frac{1}{c} \frac{\partial f}{\partial \sigma_{ij}} \quad (35)$$

and the partial derivative of  $f$  with respect to  $\sigma_{ij}$  becomes,

$$\frac{\partial f}{\partial \sigma_{ij}} = \frac{\partial f}{\partial J'_2} \frac{\partial J'_2}{\partial \sigma_{ij}} + \frac{\partial f}{\partial J'_3} \frac{\partial J'_3}{\partial \sigma_{ij}} \quad (36)$$

then by setting

$$t_{ij} = \frac{\partial J'_3}{\partial \sigma_{ij}} \quad (37)$$

the above partial derivative can be broken down into a  $J'_2$  and  $J'_3$  component. Where the parallel wrt is the second invariant is

$$\frac{\partial f}{\partial J'_2} = \frac{1}{2} \left[ J'_2 - 0.13 (J'_3)^{2/3} \right]^{-1/2} \quad (38)$$

$$\frac{\partial J'_2}{\partial \sigma_{ij}} = \sigma_{ij} \quad (39)$$

and the partial derivative wrt the third invariant

$$\frac{\partial f}{\partial J'_3} = \frac{1}{2} \left[ J'_2 - 0.13 (J'_3)^{2/3} \right]^{-1/2} \left[ -0.13 \left( \frac{2}{3} \right) (J'_3)^{-1/3} \right] \quad (40)$$

Substituting (36), (37), (38), and (39) into (35) yields

$$\frac{\partial F}{\partial \sigma_{ij}} = \frac{1}{c} \left[ \frac{1}{2 \left[ J_2' - 0.13 (J_3')^{2/3} \right]^{1/2}} \cdot \sigma_{ij}' - \frac{0.13 t_{ij}}{3(J_3')^{1/3} \left( J_2' - 0.13 (J_3')^{2/3} \right)^{1/2}} \right] \quad (41)$$

and finally substituting (41) into (34) we easily obtain

$$\dot{\epsilon}_{ij}^{vp} = \gamma \Phi(F) \left[ \frac{\sigma_{ij}}{2} - \frac{0.13 t_{ij}}{3(J_3')^{1/3}} \right] \left[ \frac{1}{J_2' - 0.13 (J_3')^{2/3}} \right]^{1/2} \quad (42)$$

For the uni-axial case under consideration in this investigation

$$s_{ij} = \begin{bmatrix} \frac{2}{3} \sigma & 0 & 0 \\ 0 & -\frac{\sigma}{3} & 0 \\ 0 & 0 & -\frac{\sigma}{3} \end{bmatrix}$$

then

$$\sigma_{11} = \frac{2}{3} \sigma \quad (43)$$

and considering the expression for  $t_{ij}$

$$t_{ij} = t_{11} = \frac{\partial J_3'}{\partial \sigma_{11}} \quad (44)$$

applying the  $J_3'$  to the above partial,  $t_{11}$  becomes

$$t_{11} = \frac{14 \sigma^2}{81} \quad (45)$$

where

$$J'_3 = \frac{2}{27} \sigma^3 \quad (46)$$

and

$$J'_2 = \frac{\sigma^2}{3} \quad (47)$$

Now with the above parameters defined for the case of uniaxial loading, the expression (43) for visco-plastic strain rate can be calculated. In this method, Rosenblatt, applied the von Mises yield condition to obtain a term which became independent of  $\frac{\partial F}{\partial \sigma_{ij}}$ .

However, by the inclusion of the third stress invariant, the expression (42) when simplified becomes

$$\dot{\epsilon}_{11} = \gamma \Phi(F) (.565) \quad (48)$$

#### 3.4. Consideration of $\Phi$ Functions

By considering the general nature of the constitutive equations the final expression relates a yield criterion and a  $\Phi$  function. The form of the function  $\Phi$  is determined analytically by considering a material's response to stress, strain, and strain rate. As was noted previously, some materials exhibit a rate sensitivity and some do not.

Several general mathematical models have been related to static stress-strain curves. These models are series expansions



which are in the form of an exponential or polynomial expression.

These functions then take the general form

$$\phi(F) = \sum_{i=1}^N A_i \left( \exp(F) - 1 \right)^i \quad (49)$$

or

$$\phi(F) = \sum_{i=1}^N B_i F^i \quad (50)$$

for

$$F = \frac{f(J_2', J_3')}{\sigma_0} - 1$$

where  $A_i$  and  $B_i$  are material constants.

Bodner and Symonds<sup>33</sup> considered a polynomial expansion where the relation between stress and strain was:

$$\phi(F) = F^\delta = \left( \frac{J_2'^{1/2}}{\sigma_0} - 1 \right)^\delta \quad (51)$$

then the form of the constitutive equations became

$$\dot{\epsilon}_{ij} = \frac{1}{2\mu} \dot{s}_{ij} + \gamma \left( \frac{J_2'^{1/2}}{\sigma_0} - 1 \right)^\delta \frac{s_{ij}}{J_2'^{1/2}}, \text{ if } J_2'^{1/2} > \sigma_0$$

$$\dot{\epsilon}_{ij} = \frac{1}{2\mu} \dot{s}_{ij}, \text{ if } J_2'^{1/2} \leq \sigma_0$$

$$\dot{\epsilon}_{11} = \frac{1}{3L} \dot{\sigma}_{11} \quad (52)$$

when elastic deformations are small in comparison with the plastic deformations, and for one dimensional states of stress, the con-

stitutive equations become

$$\dot{\epsilon} = \gamma \left( \frac{\sigma}{\sigma_0} - 1 \right)^\delta \quad (53)$$

This expression (53) is known as the Cowper-Symonds-Bodner strain rate law where  $\sigma_0 = \sqrt{3} K$ . Skolovskii<sup>34</sup> defined his strain rate law by using the assumed  $\Phi(F)$  in (51) and assigned  $\delta = 1$ .

Malvern,<sup>29</sup> assumed a material's response for differing one dimensional states of stress and strain that was in the form of an exponential:

$$\Phi(F) = \exp \left( \frac{J_2'^{\frac{1}{2}}}{\sigma_0} - 1 \right) - 1 \quad (54)$$

and the constitutive equations take the form of

$$\dot{\epsilon}_{ij} = \frac{1}{2\mu} \dot{s}_{ij} + \gamma \left( \exp \left( \frac{J_2'^{\frac{1}{2}}}{\sigma_0} - 1 \right) - 1 \right) \frac{s_{ij}}{J_2'^{\frac{1}{2}}}, \quad \text{if } J_2'^{\frac{1}{2}} > \sigma_0 \quad (55)$$

$$\dot{\epsilon}_{ij} = \frac{1}{2\mu} \dot{s}_{ij}, \quad \text{if } J_2'^{\frac{1}{2}} \leq \sigma_0$$

$$\dot{\epsilon}_{ii} = \frac{1}{3L} \dot{\sigma}_{ii}$$

then the above equations yield:

$$\epsilon = \frac{\sigma}{E} + \gamma \left\{ \exp \left( \frac{\sigma}{\sigma_0} - 1 \right) - 1 \right\} \quad (56)$$

As can be seen from the strain rate laws developed by Bodner

and Malvern, their  $\phi(F)$  functions are extractions of the general forms in (49) and (50).

Because of the analytic nature of equations (49) and (50), experimental results of stress strain curves for various strain rates were considered.<sup>5,22,24</sup> The stress strain curves for strain rates up to  $10^4 \text{ sec.}^{-1}$  were found in the literature for Aluminum, mild steel, and copper. From these data a general  $\phi(F)$  function was sought which would predict the stresses for various strains and strain rates. The exponential form of  $\phi(F)$  was applied where the strain rate in terms of  $F$  was:

$$\dot{\epsilon} = \dot{\epsilon}_o + \sum_{\alpha=1}^3 A_{\alpha} (\exp F^{\alpha} - 1); \quad F = \frac{\sigma}{\sigma_o} - 1 \quad (57)$$

where subscript (o) denotes static values, and  $A_{\alpha}$  terms are determined by a least squares fit. However, due to the nature of annealed aluminum (99.995% pure) which is highly strain rate sensitive, values of  $F$  were found to be greater than one. Then by taking the exponent of an exponential, values of the series expansion became unbounded. The unbounded problem was only encountered with the values of  $F > 1$  in this one material. But since the type of  $\phi(F)$  function desired for application to all materials, did not prove successful, another series, the power series was investigated.

For a power series, a three term expression was investigated. The general form of this expression was:

$$\ln (\dot{\epsilon}/\dot{\epsilon}_o) = \sum_{\alpha=1}^N A_{\alpha} F^{\alpha} \quad \text{for } F = \frac{\sigma}{\sigma_o} - 1 \quad (58)$$

where again, the subscript (o) denotes the static values and the coefficients  $A_{\alpha}$  are determined by applying  $\alpha$  sets of strain rate data for any strain.

Each  $A_{\alpha}$  term was found to be a function of strain and a quadratic dependence was assumed. Consequently for  $\alpha = 3$ , the coefficients of  $A_{\alpha}$  took the form,

$$\begin{aligned} A_1 &= A_{11} \epsilon^2 + B_{11} \epsilon + C_{11} \\ A_2 &= A_{22} \epsilon^2 + B_{22} \epsilon + C_{22} \\ A_3 &= A_{33} \epsilon^2 + B_{33} \epsilon + C_{33} \end{aligned} \quad (59)$$

Then by applying a least square fit to the data for various strains, the coefficients  $A_1, A_2, A_3$  were determined. Difficulty arose however when the constants  $A_{\alpha}$  were inserted into the assumed  $\Phi(F)$  function. Because a cubic equation had been assumed, the solution for  $F$ , or more appropriately the calculated values of stress gave three possible solutions. In some instances the solutions were imaginary. Since no justifiable reason could be made for incorporating the real portion of an imaginary root of  $\Phi(F)$ , the polynomial expansion was not further investigated.

Since a least square fit was applied to the experimental results a general description of this technique is presented in

Appendix B. However, because of the general nature of curve fitting to such a problem, the deviation from actual data points prompted skepticism in the final solution scheme.

Further mention should be made regarding the polynomial expansion for  $\phi(F)$ . Although real and imaginary roots were generated for various values of  $F$  and  $\dot{\epsilon}$ , reasonably good values of stress and strain rates were obtained for strain no larger than 7%. However, when larger values of strain were considered there appeared a jump in the stress-strain curve generated. Following the idea that higher order polynomial expansions would yield imaginary solutions no further attempt was made to fit a fourth order or greater expression. One and two term series were considered, however, the resulting error was considered too severe.

From the difficulties encountered in describing a general  $\phi(F)$  function with an exponential and power series expansion, it was felt that applying experimental results from stress and strain curves for various strain rates to another expression should be investigated. By considering the assumed  $\phi(F)$  functions of Perzyna<sup>7</sup>, analytic results from stress-strain curves for various strain rates held only in some cases.

Attempts to relate stress and strain rates were investigated and by applying strain rate data for lead, annealed aluminum, Al1100-0, Al1060-0, and high purity aluminum general trends were sought.

From the mathematical fits considered, the solution scheme

that best fit all the data was a particular  $\ln - \ln$  plot of stress and strain rate. The parameters which best described the data were  $\ln(e^F - 1)$  and  $\ln(\dot{\epsilon}/\dot{\epsilon}_0)$  for various strains. The equation

$$\ln(e^F - 1) = M \ln(\dot{\epsilon}/\dot{\epsilon}_0) + C \quad (60)$$

is compared to experimental data in Fig. 4. The values of  $M$  and  $C$ , which are slope and intercept respectively, were then calculated for various levels of strain.

Because a general  $\Phi(F)$  function was sought which would uniquely define a stress-strain curve for various strain rates, the values of  $M$  and  $C$  were related to strain. This relation of  $M$  and  $C$  to strain was sought since a strain term has not yet been introduced into the assumed  $\Phi(F)$  expression. For each value of strain there was a corresponding value of  $M$  and  $C$  for all the data sets. The relation of  $M$  and strain along with  $C$  and strain appeared to follow a quadratic expression where

$$\begin{aligned} M &= A_1 \epsilon^2 + B_1 \epsilon + C_1 \\ C &= A_2 \epsilon^2 + B_2 \epsilon + C_2 . \end{aligned} \quad (61)$$

The plots for annealed aluminum of  $M$  and  $C$  versus strain can be seen in Fig. 5. Although three data points were used to define the curves, since the data for all the materials considered followed the same pattern it was felt justifiable to assume a quadratic fit. Since the number of data points on the  $C$  and  $M$

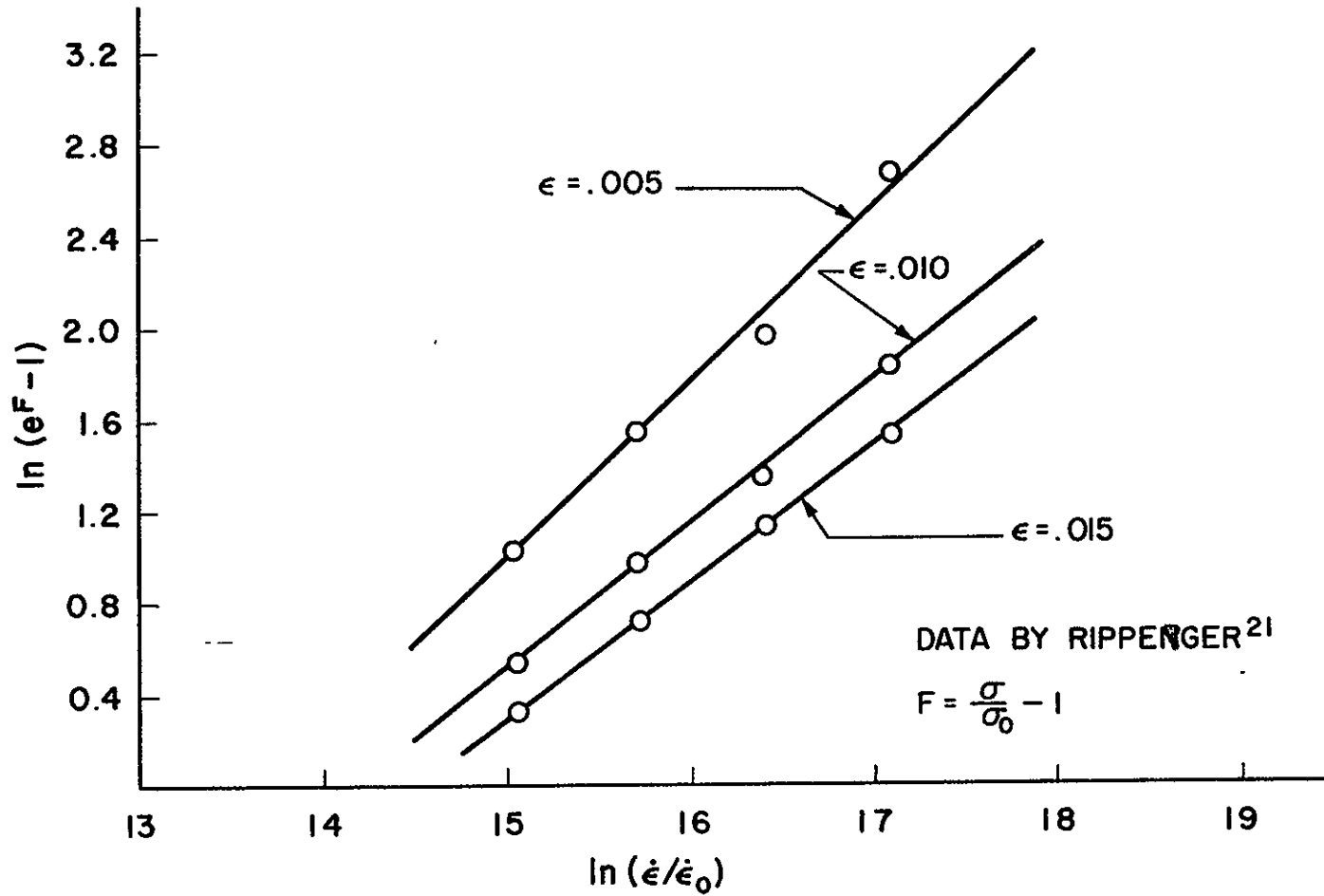


FIGURE 4 - UNI-AXIAL STRESS-STRAIN RATE EXPERIMENTS ON ANNEALED ALUMINUM

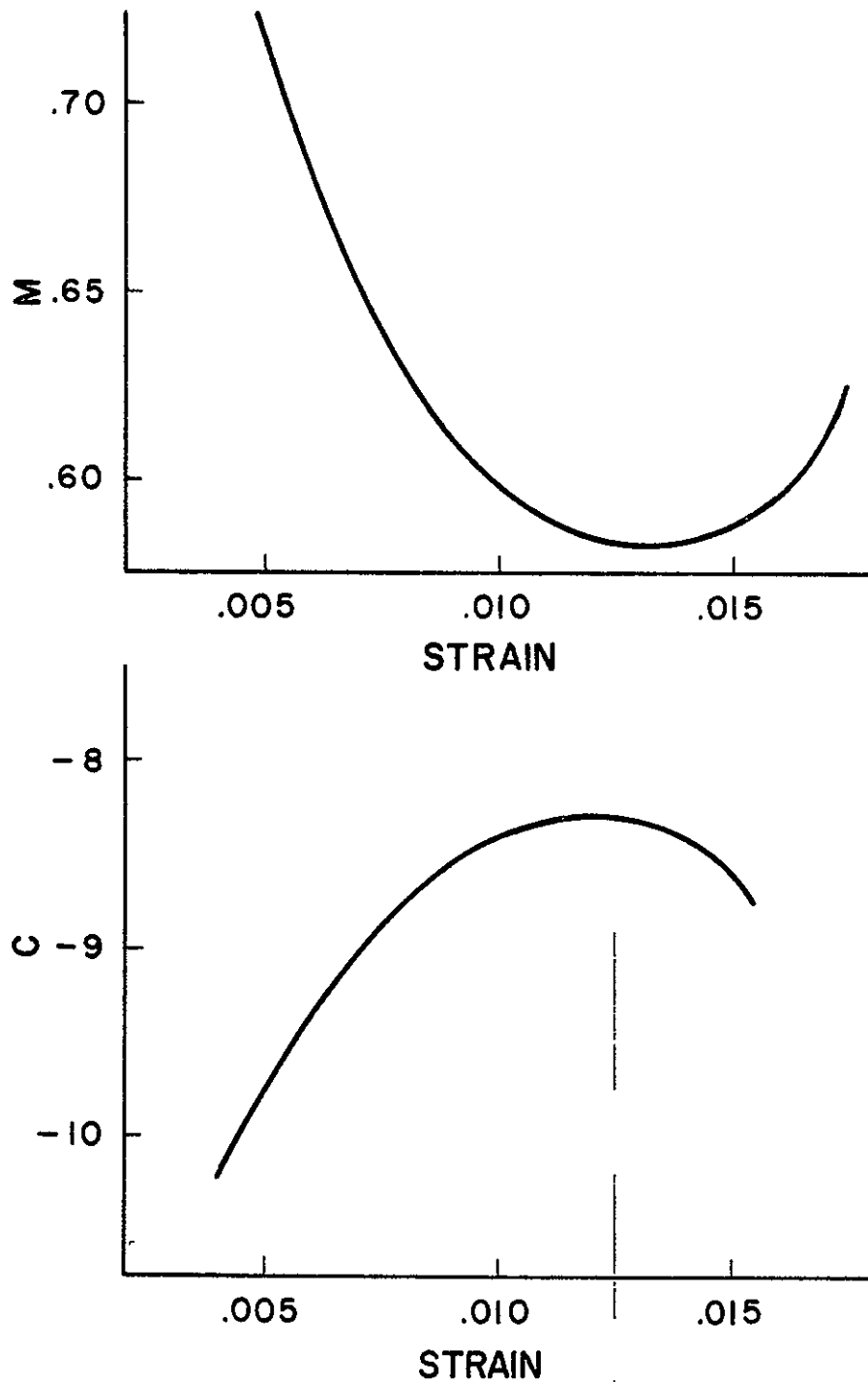


FIGURE 5 - MATERIAL PARAMETERS FOR ANNEALED ALUMINUM,  
 $\ln(e^F - 1) = M \ln \frac{\dot{\epsilon}}{\dot{\epsilon}_0} + C$



curves were small, a least square fit was made which would determine the constants  $A_1, B_1, \dots, C_2$ .

From the six calculated constants the expression to define the plastic portion of a stress-strain curve for various strain rates took the form:

$$\ln(e^F - 1) = (A_1 \epsilon^2 + B_1 \epsilon + C_1) \ln(\dot{\epsilon}/\dot{\epsilon}_0) + A_2 \epsilon^2 + B_2 \epsilon + C_2 \quad (62)$$

where

$$F = \frac{f(J_2', J_3')}{C} - 1 = \frac{\sigma}{\sigma_0} - 1 \quad (63)$$

for uni-axial loading.

The sensitivity of the six constants, can be seen from the two sets of data on 1100 Aluminum (Table 1). The strain rate data from Lindholm<sup>4</sup> and Rand<sup>5</sup>, considered in this study, differed according to values of  $F$  for similar strains and strain rates. Due to this difference in  $F$ , the corresponding constants were quite different. However, for the constants determined from each set, the computed stress for various strain and strain rates were quite close.

### 3.5. Induced Error

The error encountered by assuming a stress to strain rate expression of

TABLE 1. COMPUTED CONSTANTS FOR VARIOUS MATERIALS

MATERIAL	$A_1$	$B_1$	$C_1$	$A_2$	$B_2$	$C_2$
Al 1100-0	-2.1182	2.1434	-0.0394	-79.4931	-3.5101	-2.1708
(Rand)						
Al 1100-0	-17.8434	4.7191	-0.0045	289.2405	-77.4536	-0.5598
(Lindholm)						
Al Annealed	2429.0990	-61.0948	0.9625	-32465.5800	796.5879	-12.8006
Copper	-4.4854	0.2209	0.2120	104.8376	-9.8354	-4.3805
Lead	-0.2403	0.0803	0.0900	-20.4498	9.8762	-2.6013
High Purity Al	6.5523	-0.4771	0.3245	-102.0860	17.7017	-3.0999
Al 1060-0	-61.1543	5.2988	0.0459	512.1492	-44.3766	-2.4634

$$\ln(e^F - 1) = M \ln(\dot{\epsilon}/\dot{\epsilon}_0) + C \quad (64)$$

was considered for uni-axial loading where the form of  $F$  was

$$F = \frac{\sigma}{\sigma_0} - 1$$

and where the static values were investigated. At a static strain rate, the value of stress tends toward  $\sigma_0$  and strain rate to  $\dot{\epsilon}_0$ , that is

$$\sigma \longrightarrow \sigma_0 \text{ and } \dot{\epsilon} \longrightarrow \dot{\epsilon}_0$$

Consequently,  $F$  in the limit goes to zero and

$$\ln(e^F - 1) \Big|_{\sigma=\sigma_0} = -\infty \quad (65)$$

and the value of  $\ln(\dot{\epsilon}/\dot{\epsilon}_0)$  goes to zero. However, with the above expression in the limit the right hand side goes to the value of  $C$ , and the left hand goes to  $-\infty$ . As a result, an error was calculated in terms of  $C$  and  $\sigma_0$ . By considering equation (64) and setting

$$C = \ln C_5 \quad \text{for } C_5 < 0$$

we get

$$e^F - 1 = C_5 (\dot{\epsilon}/\dot{\epsilon}_0)^m$$

or

$$F = \ln [1 + C_5 (\dot{\epsilon}/\dot{\epsilon}_0)^m] \quad (66)$$

then by considering

$$\sigma \longrightarrow \sigma_0$$

$$\dot{\epsilon} \longrightarrow \dot{\epsilon}_0$$

the expression (66) becomes

$$\sigma = \sigma_0 + \sigma_0 \ln(1 + C_5).$$

But because  $\sigma$  goes to  $\sigma_0$ , the difference between the two stresses is the error. Or

$$\frac{\sigma - \sigma_0}{\sigma_0} = \ln(1 + C_5) \quad \text{where } C_5 = e^C \quad (67)$$

For the materials considered,  $C$  varied between  $-1.5$  and  $-9.7$  with strains up to 30%. As a result, for  $C < 0.0$  the error predicted by (69) becomes small.

### 3.6. Incorporation of $\Phi(F)$ Into the Constitutive Equations

With  $\Phi(F)$  now defined as a function of material constants  $A_1$ ,  $B_1$ , ...,  $C_2$ , for various strains, the expressions for the equivalent forms of the constitutive equations become

$$\dot{\epsilon}_{11} = \frac{1}{2\mu} \dot{S}_{11} + .565 \gamma \Phi(F) \frac{\partial F}{\partial \sigma_{11}} \quad \text{for } F > 0$$

$$\dot{\epsilon}_{11} = \frac{1}{2\mu} \dot{S}_{11} \text{ for } F \leq 0 \quad (68)$$

$$\dot{\epsilon}_{11} = \frac{1}{3L} \dot{\sigma}_{11} \text{ for}$$

where

$$\Phi(F) = \dot{\epsilon}_0 \left\{ \exp\left[\frac{\ln(\exp(F) - 1) - C}{M}\right] \right\} \quad (69)$$

and

$$M = A_1 \epsilon^2 + B_1 \epsilon + C_1$$

$$C = A_2 \epsilon^2 + B_2 \epsilon + C_2$$

### 3.7. $\Phi(F)$ for loadings other than uni-axial.

The capability of the constitutive equation to predict strain rate data for loads other than uni-axial is also considered. For the case of pure torsion, the stress matrix is

$$\tau_{ij} = \begin{bmatrix} 0 & \tau_{12} & 0 \\ \tau_{21} & 0 & 0 \\ 0 & 0 & 0 \end{bmatrix}$$

which, when considering the form of the deviator, the invariants become

$$J_1' = 0$$

$$J_2' = \tau^2 \quad (70)$$

$$J_3' = 0$$

At yield, the second invariant from pure torsion is equivalent to the second invariant from uni-axial loading by the Von Mises criterion and assuming the material is incompressible the relation

$$\tau^2_{\text{torsional}} = \frac{\sigma^2}{3}_{\text{uni-axial}} \quad \text{only at yield} \quad (71)$$

is obtained.

Consequently the form of shear stress in terms of axial stress is

$$\tau = \frac{\sigma}{\sqrt{3}} \quad (72)$$

The form of shear strain can be calculated in a similar fashion. By considering the relation

$$E = 2 G(1 + \nu) \quad (73)$$

where  $E$  is the modulus of elasticity,  $G$  the modulus of rigidity, and  $\nu$  poissons ratio. The maximum value of  $\nu$  is 0.5 at yield, which gives

$$E = 3 G .$$

Considering the relation for the modulus of elasticity

$$E = \frac{\sigma}{\epsilon}$$

becomes

$$\epsilon = \frac{\sigma}{3G} = \frac{\sqrt{3}}{3} \frac{\tau}{G}$$

and when simplifying the axial strain becomes

$$\epsilon = \frac{\gamma}{\sqrt{3}} . \quad (74)$$

With the shear stress and strain now defined in terms of uni-axial stress and strain the form of the  $\Phi(F)$  can now be considered. Considering the form of the  $\Phi(F)$  function for uni-axial loading

$$\ln(e^F - 1) = (A_1 \epsilon^2 + B_1 \epsilon + C_1) \ln(\dot{\epsilon}/\dot{\epsilon}_0) + A_2 \epsilon^2 + B_2 \epsilon + C_2 \quad (75)$$

and adapting it to a similar expression for shear loading, where for shear the  $\Phi(F)$  expression becomes

$$\ln(e^F - 1) = (A_3 \gamma^2 + B_3 \gamma + C_3) \ln(\dot{\gamma}/\dot{\gamma}_0) + A_4 \gamma^2 + B_4 \gamma + C_4$$

Now defining M and C from (74) and (75) as

$$\begin{aligned} M_{\text{uni-ax}} &= A_1 \epsilon^2 + B_1 \epsilon + C_1 \\ C_{\text{uni-ax}} &= A_2 \epsilon^2 + B_2 \epsilon + C_2 \\ M_{\text{SH}} &= A_3 \gamma^2 + B_3 \gamma + C_3 \\ C_{\text{SH}} &= A_4 \gamma^2 + B_4 \gamma + C_4 \end{aligned} \quad (76)$$

and realizing that for similar materials

$$M_{\text{uni-ax}} = M_{\text{SH}} \quad (77)$$

$$C_{\text{uni-ax}} = C_{\text{SH}}$$

the constants in uni-axial loading can also be used for torsional loading. That is for similar powers of

$$A_1 \epsilon^2 + B_1 \epsilon + C_1 = A_3 \gamma^2 + B_3 \gamma + C_3$$

the terms

$$A_1 \epsilon^2 = A_3 \gamma^2$$

$$B_1 \epsilon = B_3 \gamma$$

$$C_1 = C_3$$

From which follows

$$A_3 = A_1 \frac{\epsilon^2}{\gamma^2} = A_1 \frac{\gamma^2}{3\gamma^2} = \frac{A_1}{3}$$

In a similar manner, the forms of  $M_{\text{SH}}$  and  $C_{\text{SH}}$  become

$$M_{\text{SH}} = \frac{A_1 \gamma^2}{3} + \frac{B_1 \gamma}{\sqrt{3}} + C_1 \quad (78)$$

$$C_{\text{SH}} = \frac{A_2 \gamma^2}{3} + \frac{B_2 \gamma}{\sqrt{3}} + C_1$$

Then by applying the (78) and (77) to (75) the form of  $\Phi(F)$  becomes

$$\ln(e^F - 1) = \left( \frac{A_1 \gamma^2}{3} + \frac{B_1 \gamma}{\sqrt{3}} + C_1 \right) \ln(\dot{\gamma}/\dot{\gamma}_0) + \left( \frac{A_2 \gamma^2}{3} + \frac{B_2 \gamma}{\sqrt{3}} + C_2 \right) \quad (79)$$



The form of shear strain rate now becomes

$$\dot{\gamma} = \dot{\gamma}_0 \exp \frac{\ln(e^F - 1) - \frac{A_2 \gamma^2}{3} + \frac{B_2 \gamma}{\sqrt{3}} + C_2}{\frac{A_1 \gamma^2}{3} + \frac{B_1 \gamma}{\sqrt{3}} + C_1} \quad (80)$$

Comparison of theoretical stress-strain behavior for shear, calculated by use of the constants determined by uni-axial data, from (80) is shown in Fig. 6. Duffy et al.<sup>36</sup> considered the behavior of Al 1100-0 in pure torsion for shear strain rates up to 800 sec.<sup>-1</sup>. From their results, they established a region where shear stress and shear strain would be for strain rates on the order of 800 sec.<sup>-1</sup>.

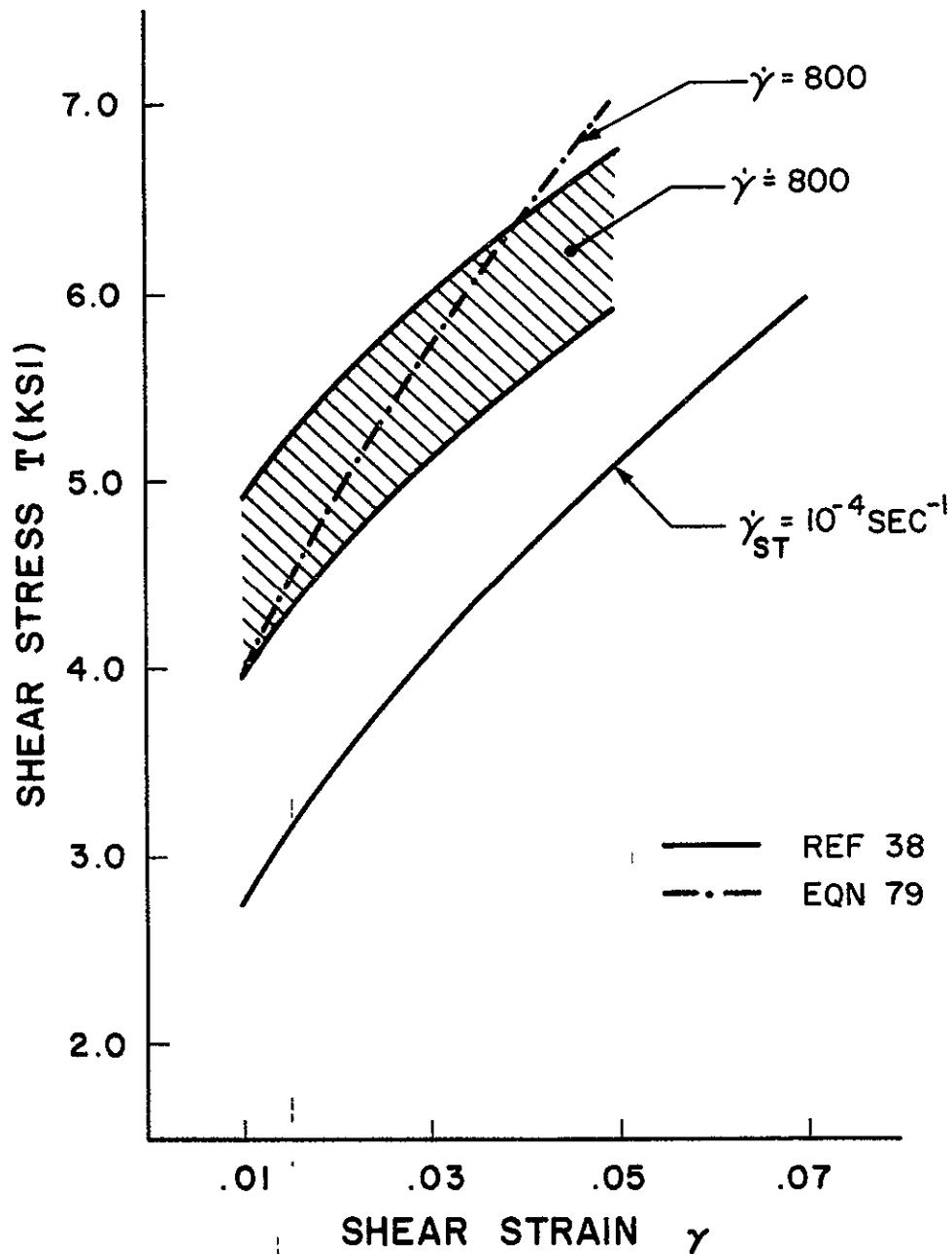


FIGURE 6 - STRESS - STRAIN BEHAVIOR IN SHEAR FOR ALUMINUM 1100-O

## CHAPTER IV

### RESULTS AND DISCUSSION

#### 4.1. Results and Concluding Remarks

The development of a rate sensitive constitutive equation has been presented which is able to describe both the elastic and plastic part of the stress-strain curve and capable of a smooth transition between the two regions. It reflects an effective change in yield stress if the material is rate sensitive and conversely, no change if the material's response is rate insensitive.

To carry out the investigation, certain steps concerning a yield criterion were established. It is from the yield criterion that the values of  $F$ , a static yield condition, are determined. This yield criterion, similar to von Mises was established on the basis of static test results and incorporated the  $J_2'$  and  $J_3'$  stress invariants. The addition of the third stress invariant  $J_3'$ , to the yield criterion required both the addition of a coefficient and an exponent to the  $J_3'$  expression. The form of yield criterion incorporated in the rate sensitive constitutive equation was

$$J_2' + k(J_3')^{2/3} = \frac{\sigma_0}{3} \left( 1.0 + \frac{k \sqrt[3]{4}}{3} \right) \quad (81)$$

where the value of the constant  $k$  of  $-0.13$  was determined from the experimental results conducted by Taylor and Quinney<sup>10</sup> for aluminum,

copper, and mild steel. On the basis of the data available, it is concluded that the effect of the third invariant is more pronounced at the combination of lower normal stresses and higher shear stresses. When the value of  $k$  is zero, the expression (81) becomes nothing more than the von Mises yield condition.

By analyzing a material's behavior experimentally, two strain sensitive material parameters can be determined. Material responses to any type of loading can be predicted by application of the constitutive equations. There are, however, two features of the equation that must be considered before determining a material's response for various strain rates. The first is determination of a static load condition,  $\sigma_0$ , and secondly, a static strain rate  $\dot{\epsilon}_0$ . By assuming the lowest strain rate given by the experimental investigations as the static rate of loading, the form of the rate sensitive constitutive equation became

$$\begin{aligned}\dot{\epsilon}_{11} &= \frac{1}{2\mu} \dot{\sigma}_{11} + (.565) \dot{\epsilon}_0 \left\{ \exp \right. \\ &\quad \left. \left[ \frac{\ln(e^F - 1) - (A_2 \epsilon^2 + B_2 \epsilon + C_2)}{A_1 \epsilon^2 + B_1 \epsilon + C_1} \right] \right\} \frac{\partial F}{\partial \sigma_{11}} \text{ for } F > 1 \\ &\quad \quad \quad (82) \\ \dot{\epsilon}_{11} &= \frac{1}{2\mu} \dot{\sigma}_{11} \quad \quad \quad \text{for } F \leq 1 \\ \dot{\epsilon}_{11} &= \frac{1}{3L} \dot{\sigma}_{11}\end{aligned}$$

for uni-axial loading where

$$F = \frac{\sigma}{\sigma_0} - 1.$$

The constants determined for various materials are given in Table 1. In addition, detailed comparisons of theory and experiment are given graphically in Appendix C. In some instances large strain rates for highly rate sensitive materials depict significant changes in stress for a given strain, as for example high purity aluminum. Likewise, little or no change in effective stress is displayed for rate insensitive materials such as copper.

The development of the constitutive equations to account for torsional loadings is also made by applying the von Mises criterion of  $\tau = \frac{\sigma}{\sqrt{3}}$  and  $\gamma = \sqrt{3} \epsilon$  and using the constants in Table 1, the strain rate sensitive constitutive equations can account for dynamic shear loadings. Comparison of predicted values with the experimental results of Ref. 36 is made for Aluminum 1100-0 at a shear strain rate of  $800 \text{ sec}^{-1}$ . Good agreement exists for low shear strains, however, for large shear strains there seems to be some discrepancy. This discrepancy could be due to the difference in static strain rates used to calculate the constants and that used in the experimental torsional tests. Also as was noted in Ref. 36, the experimental results for dynamic torsional loadings at high strain rates do not follow the values experimentally obtained by Ref. 4 for high strains. Scatter in test results of Ref. 36 for shear strain rates of  $800 \text{ sec}^{-1}$  can be seen in Fig. 6. However for low shear strains,  $.02 < \gamma < .05$ , the predicted stresses

and strains by using (82) with the results obtained from Ref. 36 are in reasonably close agreement.

Small discrepancies arise in the comparison of experiments and theoretical stress for various strain rates due to the incorporation of scattered data. In the experimental study concerning lead, the scatter of stresses for strain rates of  $10^4 \text{ sec}^{-1}$  affected the determination of the six constants. Consequently, in the comparison of the theoretical and experimental stress an error might be deduced from each of the stress readings. However, to predict a trend for this material, the theoretical results seem plausible.

For the  $\Phi(F)$  function developed, the error introduced by considering the limiting values of stress and strain rate where  $\sigma$  tends to  $\sigma_0$  and  $\dot{\epsilon}$  to  $\dot{\epsilon}_0$  becomes

$$\frac{\sigma - \sigma_0}{\sigma_0} = \ln \{ \exp (A_2 \epsilon^2 + B_2 \epsilon + C_2) + 1 \} \quad (83)$$

where the exponent of the exponential is always negative.

The use of the strain rate sensitive constitutive equation to predict stresses for various strain rates on the order of those encountered during hypervelocity impact is now possible. However, comparison of theoretical values to experimental data is not possible at the present time, since there is no rate testing device which can generate strain rates on the order of  $10^6 \text{ sec}^{-1}$ .

The incorporation of rate sensitivity into the constitutive

equation adapts the constitutive equations to account for various strain rates. By applying the constitutive equations developed here, to a material's response at hypervelocity impact, a legitimate method is now available to determine strength effects of various materials to different rates of loading.

## REFERENCES

- 1 Heyda, J. F., and Riney, T. D., "Peak Pressures In Thick Targets Generated by Reduced Density Projectiles", NASA CR-609.
- 2 Wilkins, M. L., "Calculations of Elastic-Plastic Flow," Methods In Computational Physics, Vol. 3, Academic Press, New York, 1964, p. 226.
- 3 Harlow, F. H., Los Alamos Scientific Lab. Rept. LA-2301, 1965.
- 4 Lindholm, U. S., and Yeakley, L. M., "High Strain-Rate Testing: Tension and Compression," Experimental Mechanics, Jan. 1968, pp. 1-9.
- 5 Rand, J. L., "An Analysis of the Split Hopkinson Pressure Bar," NOLTR 67-156; U. S. Naval Ordnance Laboratory, Silver Spring, Maryland, 1967, p. 43.
- 6 Hauser, F. E., Simmons, J. A., and Dorn, J. E., "Strain Rate Effects in Plastic Wave Propagation," Response of Metals to High Velocity Deformation, Metallurgical Society Conferences, Vol. 9, New York, 1960, p. 105.
- 7 Perzyna, P., "The Constitutive Equation for Rate Sensitive Plastic Materials," Quarterly of Applied Mathematics, Vol. 20, No. 4, 1964, pp. 321-332.
- 8 Cristescu, N., Dynamic Plasticity, John Wiley & Sons, Inc., New York, 1967, pp. 101-119.
- 9 Hopkinson, B., Proceedings of the Royal Society, Series A. Vol. 74, London, 1905, pp. 498-506.
- 10 Taylor, G.I., and Quinney, H., "The Plastic Distortion of Metals," Philosophical Transactions of the Royal Society, London, Series A., Nov. 13, 1931, pp. 323-362.
- 11 Drucker, D.C., "Relation of Experiments to Mathematical Theories of Plasticity," Journal of Applied Mechanics, Dec. 1949, pp. 349-357.
- 12 Naghdi, P.M., Essenburg, F., and Koff, W., "An Experimental Study of Initial and Subsequent Yield Surfaces in Plasticity", Journal of Applied Mechanics, June 1958, pp. 201-209.



- 13 Cook, P.M., "Proc. Conference on Properties of Materials at High Rates of Strain", London, April 30-May 2, 1957, pp. 86-97.
- 14 Kolsky, H., and Douch, L.S., Journal of the Mechanics and Physics of Solids, Vol. 10, 1962, pp. 195-223.
- 15 Bell, J.F., "Study of Initial Conditions in Constant Velocity Impact," Journal of Applied Physics, Vol. 31, No. 12, Dec. 1960, pp. 2188-2195.
- 16 Alter, B.E., and Curtis, C.W., "Effect of Strain Rate on the Propagation of a Plastic Strain Pulse Along a Lead Bar," Journal of Applied Physics, Vol. 27, No. 9, Sept. 1956, pp. 1079-1085.
- 17 Baron, H.G., "Stress/Strain Curves of Some Metals and Alloys," Journal of the Iron and Steel Institute, April 1956, pp. 354-365.
- 18 Chiddister, J.L., and Malvern, L.E., "Compression Impact Testing of Aluminum at Elevated Temperatures" Experimental Mechanics, April 1963, pp. 81-90.
- 19 McLellan, C.L., "Constitutive Equations for Mechanical Properties of Structural Materials," AIAA Journal, Vol. 5, No. 3, March 1967, pp. 446-450.
- 20 Green, S.J., Maiden, C.J., "Compressive Strain Rate Tests on Six Selected Materials at Strain Rates from  $10^{-3}$  to  $10^4$  sec.<sup>-1</sup>," Journal of Applied Mechanics, Sept. 1966, pp. 496-504.
- 21 Karnes, C.H., and Ripperger, E.A., "Strain Rate Effects In Cold Worked High Purity Aluminum," Journal of the Mechanics and Physics of Solids, Vol. 14, No. 2, March 1966, pp. 75-88.
- 22 Lindholm, U.S., "Some Experiments in Dynamic Plasticity Under Combined Stress," Mechanical Behavior of Materials Under Dynamic Loads, U.S. Lindholm Ed., New York, N.Y., 1967, pp. 77-95.
- 23 Brown, G.M., "Inelastic Deformation of An Aluminum Alloy Under Combined Stress at Elevated Temperature," Journal of Mechanics and Physics of Solids, Vol. 18, pp. 383-396.
- 24 Lindholm, U.S., "Dynamic Deformation of Metals," Behavior of Materials Under Dynamic Loading, ASME, 1965, pp. 42-53.

- 25 Bell, J. F., "The Dynamic Plasticity of Metals at High Strain Rates: An Experimental Generalization," Behavior of Metals Under Dynamic Loading; ASME, 1965, pp. 19-38.
- 26 Butcher, B. M., and Karnes, C. H., "Strain Rate Effects in Metals," Journal of Applied Physics, Vol. 37, No. 1, January 1966.
- 27 Rakhmatulin, K. A., "Propagation of A Wave of Unloading," Prikl. Mat. Mekh. 9, 91 (1945), (Office of Naval Research, Translation No. 2), Brown University, Providence, 1948.
- 28 von Karman, T., and Duwez, P. E., "The Propagation of Plastic Deformation in Solids," The Journal of Applied Physics, Vol. 21, 1950, pp. 987-994.
- 29 Malvern, L. E., "The Propagation of Longitudinal Waves of Plastic Deformation In a Bar Exhibiting a Strain-Rate Effect," Journal of Applied Mechanics, Vol. 18, 1951, pp. 203-207.
- 30 Wood, D. S., "On Longitudinal Plane Waves of Elastic-Plastic Strain in Solids," Journal of Applied Mechanics, Dec. 1952, pp. 521-525.
- 31 Hohenemser, K., and Prager, W., "Über die Ansätze der Mechanik isotroper Kontinua", Zeitschrift für Angew. Math. Phys., Vol. 12, 1932, pp. 216-226.
- 32 Rosenblatt, M., Analytical Study of Strain Rate Effects in Hypervelocity Impact, NASA CR-61323, Jan. 1970, pp. 10-15.
- 33 Bodner, S. R. and Symonds, P. S., "Plastic Deformation in Impact and Impulsive Loading of Beams," Plasticity, Pergamon Press, New York, 1960, pp. 488-500.
- 34 Sokolovskii, V. V., "Propagation of Elastic-Visco-Plastic Waves in Bars," Prikl. Mat. Mekh., Vol. 12, 1948, pp. 261-280.
- 35 Jones, A. H., Maiden, C. J., Green, S. J., and Chin, H., "Prediction of Elastic-Plastic Wave Profiles in Aluminum 1060-0 Under Uni-axial Strain Loading," Mechanical Behavior of Metals Under Dynamic Loads, Publ. Springer - Verlag, New York, Inc. 1968, pp. 254-259.
- 36 Duffy, J., Campbell, J. D., Hawley, R. H., "On the Use of a Torsional Split Hopkinson Bar to Study Rate Effects in 1100-0 Aluminum," Journal of Applied Mechanics, March 1971, pp. 83-91.
- 37 Kolsky, H., Stress Waves in Solids, Dover Publications, New York, 1963, pp. 150-158.

## APPENDIX A

## A.1. Development of the Stress Deviator

In the development of the constitutive equations, the incorporation of the second and third stress invariants is made. By using the notation of  $J_2$  and  $J_3$  as the second and third invariants, the nomenclature of the yield criterion is simplified.

Considering an elemental volume which has nine stresses acting on it, the stress tensor can be defined as

$$\sigma_{ij} = \begin{bmatrix} \sigma_{11} & \sigma_{12} & \sigma_{13} \\ \sigma_{21} & \sigma_{22} & \sigma_{23} \\ \sigma_{31} & \sigma_{32} & \sigma_{33} \end{bmatrix} \quad (\text{A-1})$$

however the form of  $\sigma_{ij}$  is such that it can be broken down into two parts. One part deals with the change in shape and the other with the change in volume. That is

$$\begin{array}{lcl} \text{(Stress Tensor)} & = & \text{Change in Shape} + \text{Change in Volume} \\ & & \text{(deviatoric tensor)} \quad \text{(hydrostatic tensor)} \end{array}$$

$$\begin{bmatrix} \sigma_{11} & \sigma_{12} & \sigma_{13} \\ \sigma_{21} & \sigma_{22} & \sigma_{23} \\ \sigma_{31} & \sigma_{32} & \sigma_{33} \end{bmatrix} = \begin{bmatrix} \sigma_{11} - p & \sigma_{12} & \sigma_{13} \\ \sigma_{21} & \sigma_{22} - p & \sigma_{23} \\ \sigma_{31} & \sigma_{32} & \sigma_{33} - p \end{bmatrix} + \begin{bmatrix} p & 0 & 0 \\ 0 & p & 0 \\ 0 & 0 & p \end{bmatrix}$$

(A-2)

where

$$p = \frac{\sigma_{11} + \sigma_{22} + \sigma_{33}}{3} \quad (\text{A-3})$$

If the notation for the deviatoric tensor is  $\sigma'_{ij}$  and for the hydrostatic tensor  $\sigma''_{ij}$ , then the expression for the invariants of the stress deviators become

$$J'_1 = \sigma'_{ii}$$

$$J'_2 = \frac{1}{2} (\sigma'_{ij} \sigma'_{ji}) \quad (\text{A-4})$$

$$J'_3 = \frac{1}{3} (\sigma'_{ij} \sigma'_{jk} \sigma'_{ki})$$

where  $\sigma'_{ij}$  is the substitution of (A-3) into the deviatoric portion of (A-2). The form of  $\sigma'_{ij}$  becomes

$$\sigma'_{ij} = \begin{bmatrix} \frac{2\sigma_{11} - \sigma_{22} - \sigma_{33}}{3} & \sigma_{12} & \sigma_{13} \\ \sigma_{21} & \frac{2\sigma_{22} - \sigma_{11} - \sigma_{33}}{3} & \sigma_{23} \\ \sigma_{31} & \sigma_{32} & \frac{2\sigma_{33} - \sigma_{11} - \sigma_{22}}{3} \end{bmatrix} \quad (\text{A-5})$$

The above tensor becomes symmetric if the non-polar form of stress is considered. By considering the components of the tensor (A-5) and applying them to (A-4) the deviatoric stress invariants greatly simplify. The deviator of the first invariant becomes

$$J'_1 = \sigma'_{11} + \sigma'_{22} + \sigma'_{33} = 0 \quad (\text{A-6})$$

The second invariant of the stress deviator is

$$\begin{aligned} J'_2 &= \frac{1}{2} \{ \sigma'_{11} \sigma'_{11} + \sigma'_{12} \sigma'_{21} + \sigma'_{13} \sigma'_{31} + \sigma'_{21} \sigma'_{12} + \sigma'_{22} \sigma'_{22} \\ &\quad + \sigma'_{23} \sigma'_{32} + \sigma'_{31} \sigma'_{13} + \sigma'_{32} \sigma'_{23} + \sigma'_{33} \sigma'_{33} \} \\ \text{or } J'_2 &= \frac{1}{2} \left\{ \left( \frac{2\sigma'_{11} - \sigma'_{22} - \sigma'_{33}}{3} \right)^2 + \frac{2\sigma'_{22} - \sigma'_{11} - \sigma'_{33}}{3} \right. \\ &\quad \left. + \left( \frac{2\sigma'_{33} - \sigma'_{22} - \sigma'_{11}}{3} \right)^2 + 2\sigma'^2_{12} + 2\sigma'^2_{13} + 2\sigma'^2_{23} \right\}. \end{aligned}$$

Then with further simplification and considering the symmetry of the tensor, the second invariant becomes

$$\begin{aligned} J'_2 &= \left\{ \frac{1}{3} (\sigma'^2_{11} + \sigma'^2_{22} + \sigma'^2_{33}) - \frac{1}{3} (\sigma'_{11} \sigma'_{22} + \sigma'_{11} \sigma'_{33} + \sigma'_{22} \sigma'_{33}) \right. \\ &\quad \left. + \sigma'^2_{12} + \sigma'^2_{13} + \sigma'^2_{23} \right\} \end{aligned}$$

For the uni-axial case considered in this research, the final form of  $J'_2$  becomes

$$J'_2 = \frac{1}{3} \sigma'^2_{11} \quad (\text{A-7})$$

Consideration of the third invariant of the deviator yields:

$$J'_3 = \{\sigma'_{11} \sigma'_{22} \sigma'_{33} + \sigma'_{12} \sigma'_{23} \sigma'_{31} + \sigma'_{13} \sigma'_{32} \sigma'_{21} \\ - \sigma'_{31} \sigma'_{13} \sigma'_{22} - \sigma'_{12} \sigma'_{21} \sigma'_{33} - \sigma'_{11} \sigma'_{32} \sigma'_{23}\}$$

or

$$J'_3 = [(\frac{2\sigma_{11} - \sigma_{22} - \sigma_{33}}{3})(\frac{2\sigma_{22} - \sigma_{11} - \sigma_{33}}{3})(\frac{2\sigma_{33} - \sigma_{11} - \sigma_{33}}{3}) \\ + \sigma_{12} \sigma_{23} \sigma_{31} + \sigma_{13} \sigma_{32} \sigma_{21} - \sigma_{31} \sigma_{13} (\frac{2\sigma_{22} - \sigma_{11} - \sigma_{33}}{3}) \\ - \sigma_{12} \sigma_{23} \sigma_{31} + \sigma_{13} \sigma_{32} \sigma_{21} - \sigma_{31} \sigma_{13} (\frac{2\sigma_{22} - \sigma_{11} - \sigma_{33}}{3}) \\ - \sigma_{12} \sigma_{21} (\frac{2\sigma_{33} - \sigma_{11} - \sigma_{22}}{3}) - \sigma_{23} \sigma_{32} (\frac{2\sigma_{11} - \sigma_{22} - \sigma_{33}}{3})]$$

Then for uni-axial loading, the expression becomes

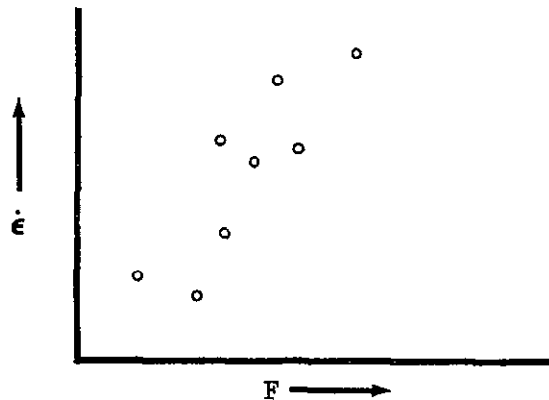
$$J'_3 = \frac{2}{27} \sigma_{11}^3 \quad (A-8)$$

## APPENDIX B

## Least Square Fit To Data

Least square curve fitting amounts to determining the curve passing through the average of  $x$  and the average of  $y$ , i.e., the center of gravity of the data, with the incremental slope  $m$ , which minimizes the sum of the squares of the deviation of the data from the curve.

Assume for the present problem, that we seek the best fit by minimizing the square of the deviation from a set of experimental points and which satisfy the condition  $\dot{\epsilon} = 0$  and  $F = 0$  at the origin exactly. Also assume that we have  $M$  pairs of data  $(\dot{\epsilon}_i, F_i)$



and we wish to fit this data with some analytic expression

$$y = \dot{\epsilon}_0 + \sum_{n=1}^K A_n f_n(F)$$

The function  $f_n$  should be chosen so that:

$$f_n(0) = 0 \quad \text{for all } 1 \leq n \leq K$$

Possible functions which satisfy this condition are

$$1.) \quad f_n(F) = F^n$$

$$2.) \quad f_n(F) = e^{F^n} - 1$$

$$3.) \quad f_n(F) = (e^F - 1)^n$$

$$4.) \quad f_n(F) = F\{G_n(F)\} \quad \text{except if } G = \frac{1}{F}$$

The difference between the predicted and experimental  $i$ th point is:

$$y(F_i) - \dot{\epsilon}_i = \delta_i$$

Now define the residual as the sum of the squares of the differences

$$R = \sum_{i=1}^M \delta_i^2 = \sum_{i=1}^M [Y(F_i) - \ln \dot{\epsilon}_i]^2$$

where  $R = R(A_n)$ . In order to minimize  $R$ , we write  $K$  equations in the form

$$\frac{\partial R}{\partial A_n} = 0 \quad n = 1, 2, 3, \dots, K$$

thus

$$\frac{\partial}{\partial A_n} \sum_{i=1}^M [Y_i - \ln \dot{\epsilon}_i]^2 = \sum_{i=1}^M 2\{Y(F_i) - \ln \dot{\epsilon}_i\} \frac{\partial Y(F_i)}{\partial A_n} = 0$$



where

$$\frac{\partial y}{\partial A_n} = f_n(F_i)$$

Substitution for  $y(F_i)$  yields:

$$\sum_{i=1}^M f_n(F_i) \sum_{n=1}^K A_n f_n(F_i) = \sum f_n(F_i) \ln(\dot{\epsilon}_i/\dot{\epsilon}_0)$$

This can be further simplified by considering:

$$\sum_{n=1}^K A_n \sum_{i=1}^M f_n(F_i) f_n(F_i)$$

From the above expression parameters such as

$$K_{pq} = \sum_{i=1}^M f_p(F_i) f_q(F_i)$$

and

$$C_p = \sum_{n=1}^M f_p(F_i) \ln(\dot{\epsilon}_i/\dot{\epsilon}_0)$$

can be defined. Then the simplified expression

$$K_{pq} A_q = C_p$$

follows, and if put into matrix form

$$[K] \{A\} = \{C\}$$

the values of  $\{A\}$  can be made by inverting the matrix  $[K]$ , or

$$\{A\} = [K]^{-1} \{C\}$$

which yield K values of  $A_q$ .

For a sample calculation, consider the quadratic expression

$$Y = A_0 + A_1 X_1 + A_2 X_2$$

where

$$X_1 = F$$

$$X_2 = F^2$$

and four sets of data points for Y and F: (11,1), (21,2), (29,3), (36,4). Then

$$\sum_n Y = n A_0 + A_1 \sum_n X_1 + A_2 \sum_n X_2$$

$$\sum_n X_1 Y = A_0 \sum_n X_1 + A_1 \sum_n X_1 X_1 + A_2 \sum_n X_1 X_2$$

$$\sum_n X_2 Y = A_0 \sum_n X_2 + A_1 \sum_n X_1 X_2 + A_2 \sum_n X_2 X_2$$

and by using matrix notation

$$\begin{bmatrix} n & \sum_n X_1 & \sum_n X_2 \\ \sum_n X_1 & \sum_n X_1 X_1 & \sum_n X_1 X_2 \\ \sum_n X_2 & \sum_n X_1 X_2 & \sum_n X_2 X_2 \end{bmatrix} \cdot \begin{bmatrix} A_0 \\ A_1 \\ A_2 \end{bmatrix} = \begin{bmatrix} \sum_n Y \\ \sum_n X_1 Y \\ \sum_n X_2 Y \end{bmatrix}$$

Considering the four sets of data, the above expression becomes

$$\begin{bmatrix} (4) & (1+2+3+4) & (1+4+9+16) \\ (1+2+3+4) & (1+4+9+16) & (1+8+27+64) \\ (1+4+9+16) & (1+8+27+64) & (1+16+81+256) \end{bmatrix} \cdot \begin{bmatrix} A_0 \\ A_1 \\ A_2 \end{bmatrix} = \begin{bmatrix} (11+21+29+36) \\ (11+42+87+144) \\ (11+84+261+576) \end{bmatrix}$$

and the expression for the constants to the expression

$$Y = A_0 + A_1 X_1 + A_2 X_2$$

becomes

$$\begin{bmatrix} A_0 \\ A_1 \\ A_2 \end{bmatrix} = \begin{bmatrix} 4 & 10 & 30 \\ 10 & 30 & 100 \\ 30 & 100 & 354 \end{bmatrix}^{-1} \cdot \begin{bmatrix} 97 \\ 284 \\ 932 \end{bmatrix}$$

where by

$$A_0 = -0.25$$

$$A_1 = 12.05$$

$$A_2 = -0.75$$

## APPENDIX C

## Strain Rate Data

Rate sensitive data for various stresses and strains were necessary to carry out the investigation of the constitutive equations. Due to the lack of an available testing device, published data in this area were consulted. Because a general rate sensitive constitutive equation was sought, various materials were considered. The materials considered were lead, copper, high purity aluminum, annealed aluminum, and 1100-0 Aluminum.

The data consulted consisted only of uni-axial loading and generally considered strains no greater than 15%. The strain rates given were generally no greater than  $10^4 \text{ sec}^{-1}$ . Once the determination of stress and strain rates for various strains was made, the values of  $F$  and  $\dot{\epsilon}/\dot{\epsilon}_0$  were computed. Utilizing these computed values, the constants  $A_1, B_1, C_1, \dots, C_2$  required for the following equation were empirically determined by a least squares procedure developed in Appendix B:

$$\ln(e^F - 1) = (A_1 \epsilon^2 + B_1 \epsilon + C_1) \ln(\dot{\epsilon}/\dot{\epsilon}_0) + (A_2 \epsilon^2 + B_2 \epsilon + C_2) \quad (C-1)$$

These material parameters are listed in Table 1 for each material. In Fig. 7, a comparison of experimental data and the theoretical prediction for Annealed Aluminum at various strain rates is shown. It can be seen that a significant error is introduced in the

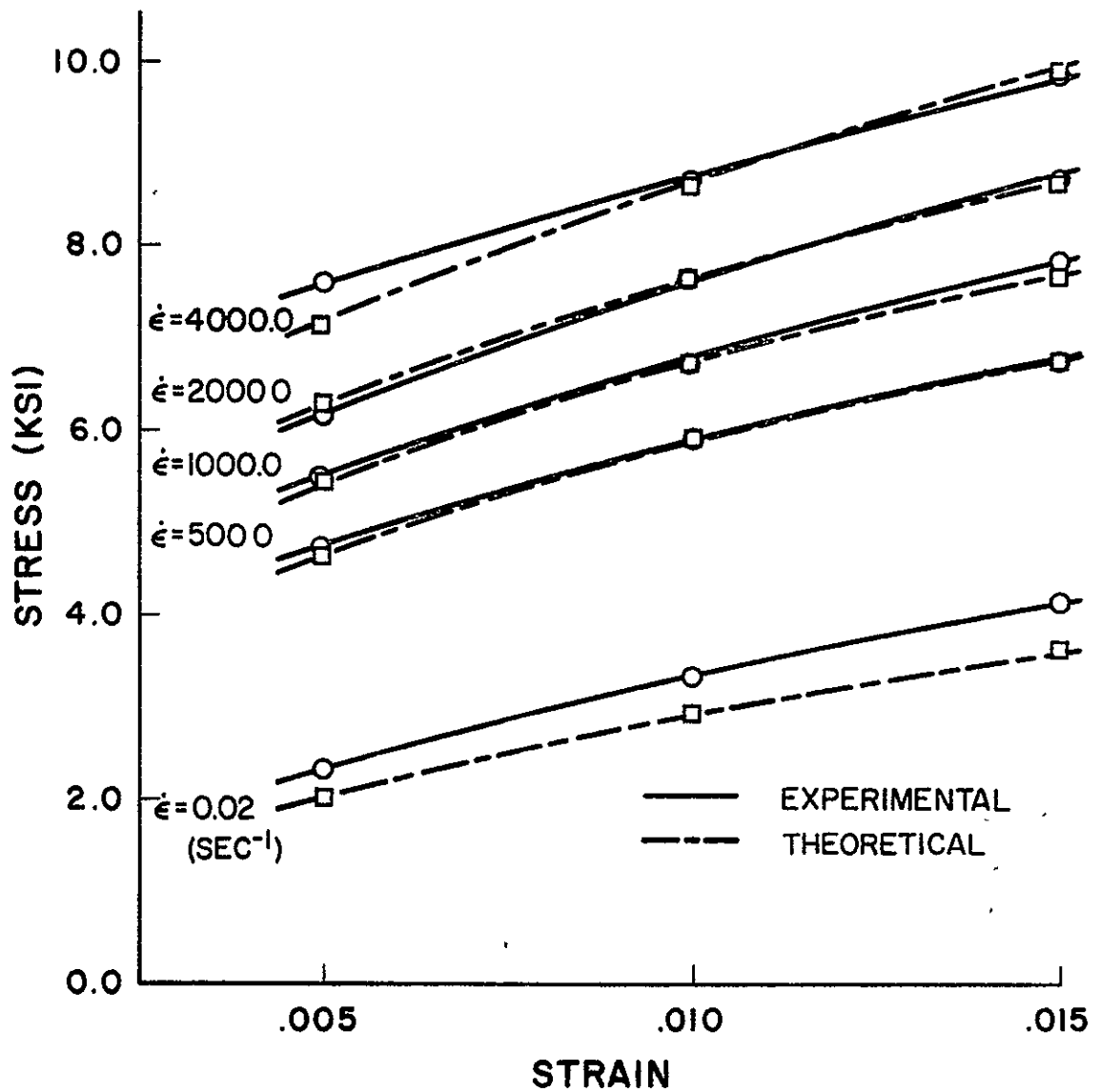


FIGURE 7 – EXPERIMENTAL AND THEORETICAL  
RATE SENSITIVITY FOR  
ANNEALED AL (99.995% PURE)

neighborhood of the static strain rate.

Equation C-1 is plotted for various constant strain rates in Figures 8 through 14. The rates considered vary from static values to those encountered in the hypervelocity impact process.

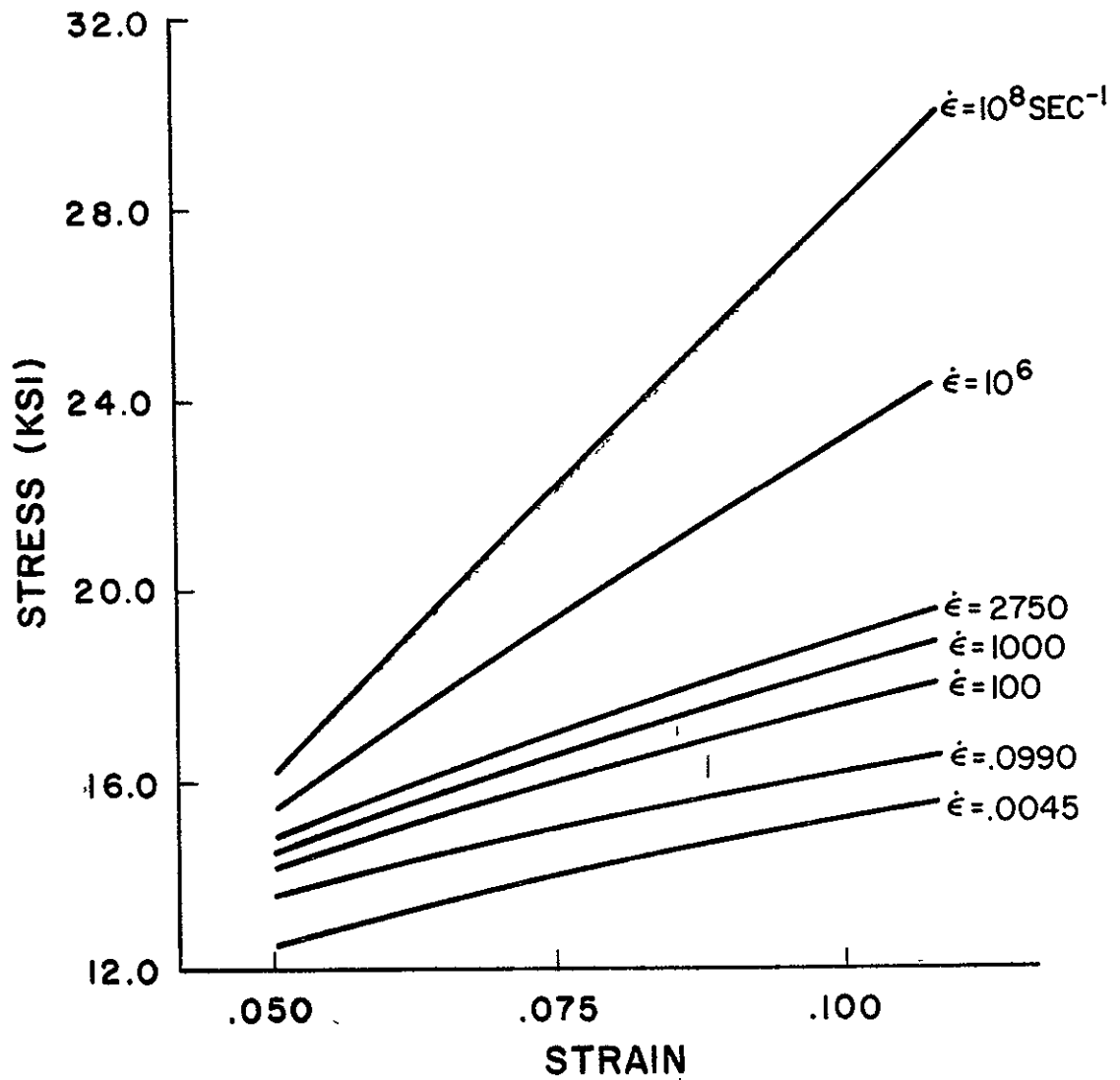


FIGURE 8 - DYNAMIC RESPONSE OF ALUMINUM 1100-O (RAND)

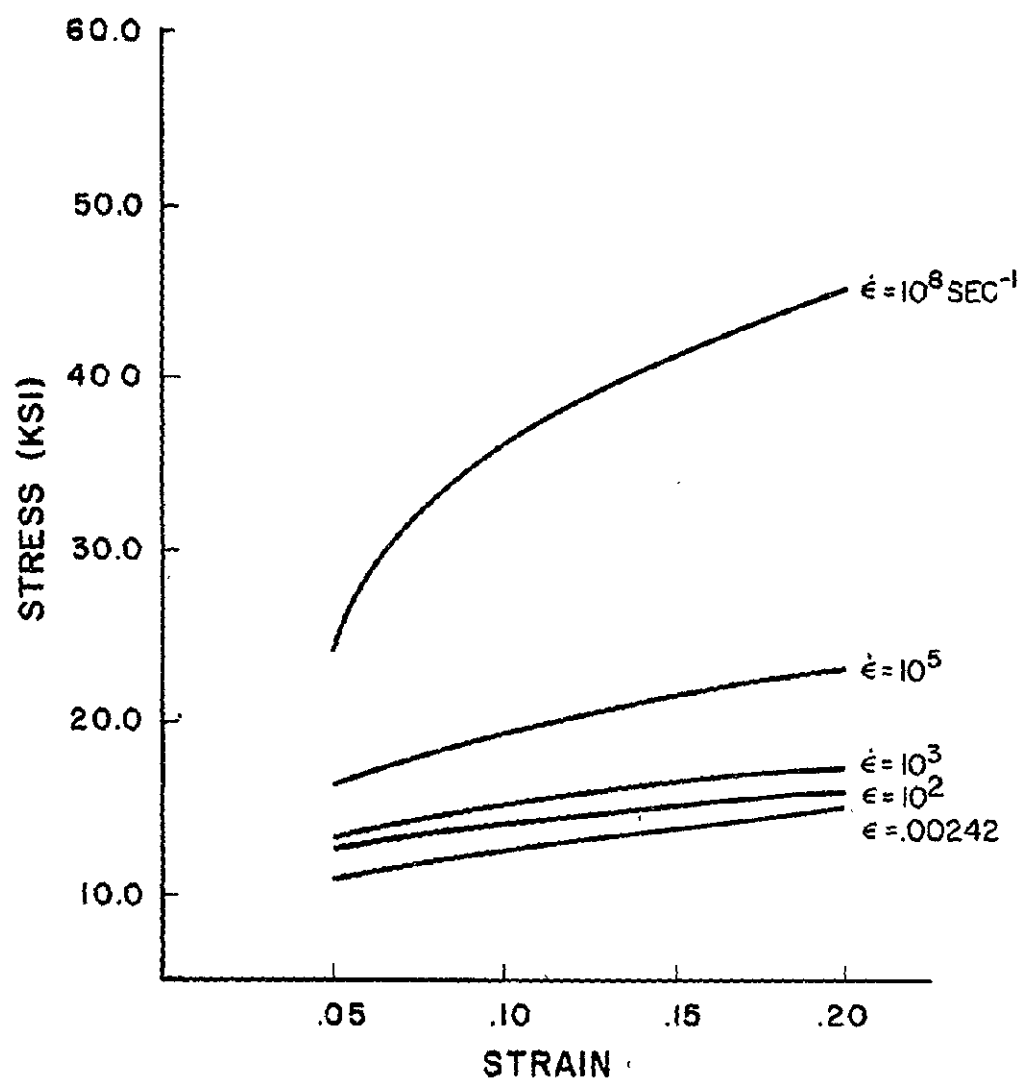


FIGURE 9 - DYNAMIC RESPONSE OF  
ALUMINUM 1100-O (LINDHOLM)



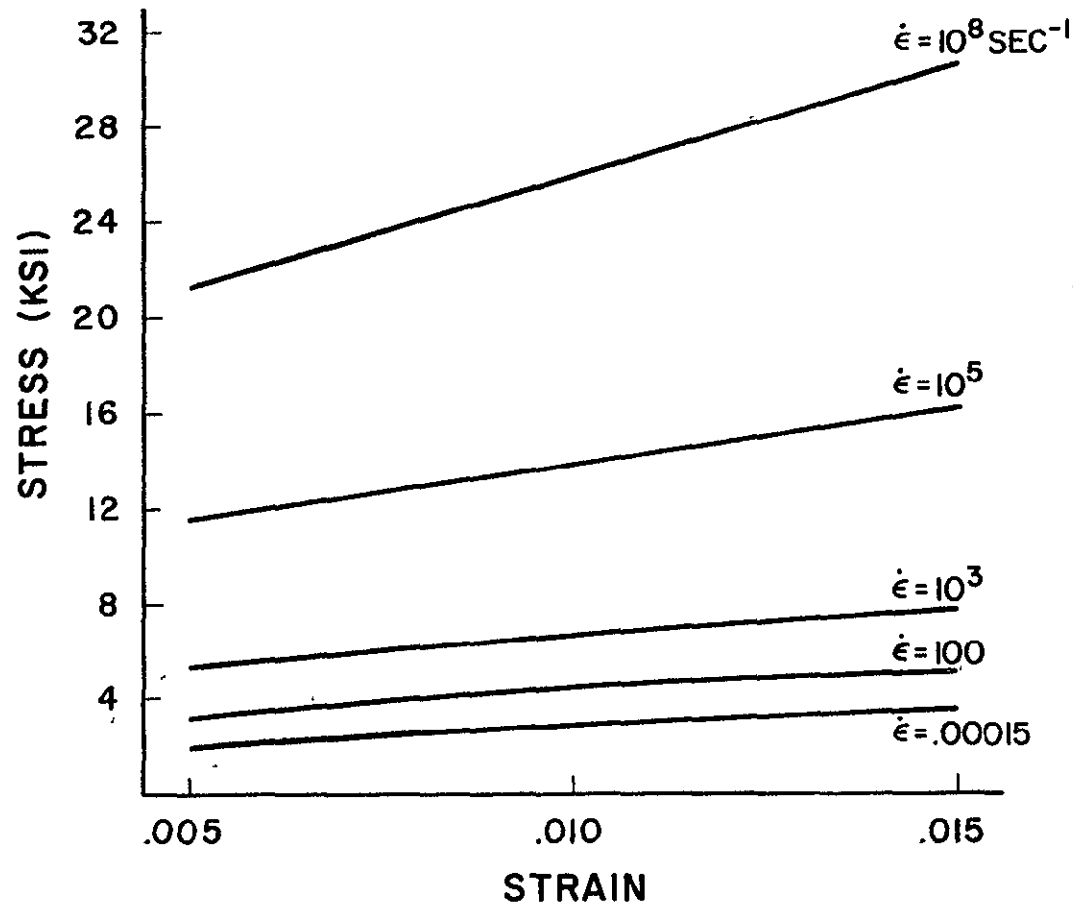


FIGURE 10 – DYNAMIC RESPONSE OF ANNEALED ALUMINUM (99.995 % PURE)

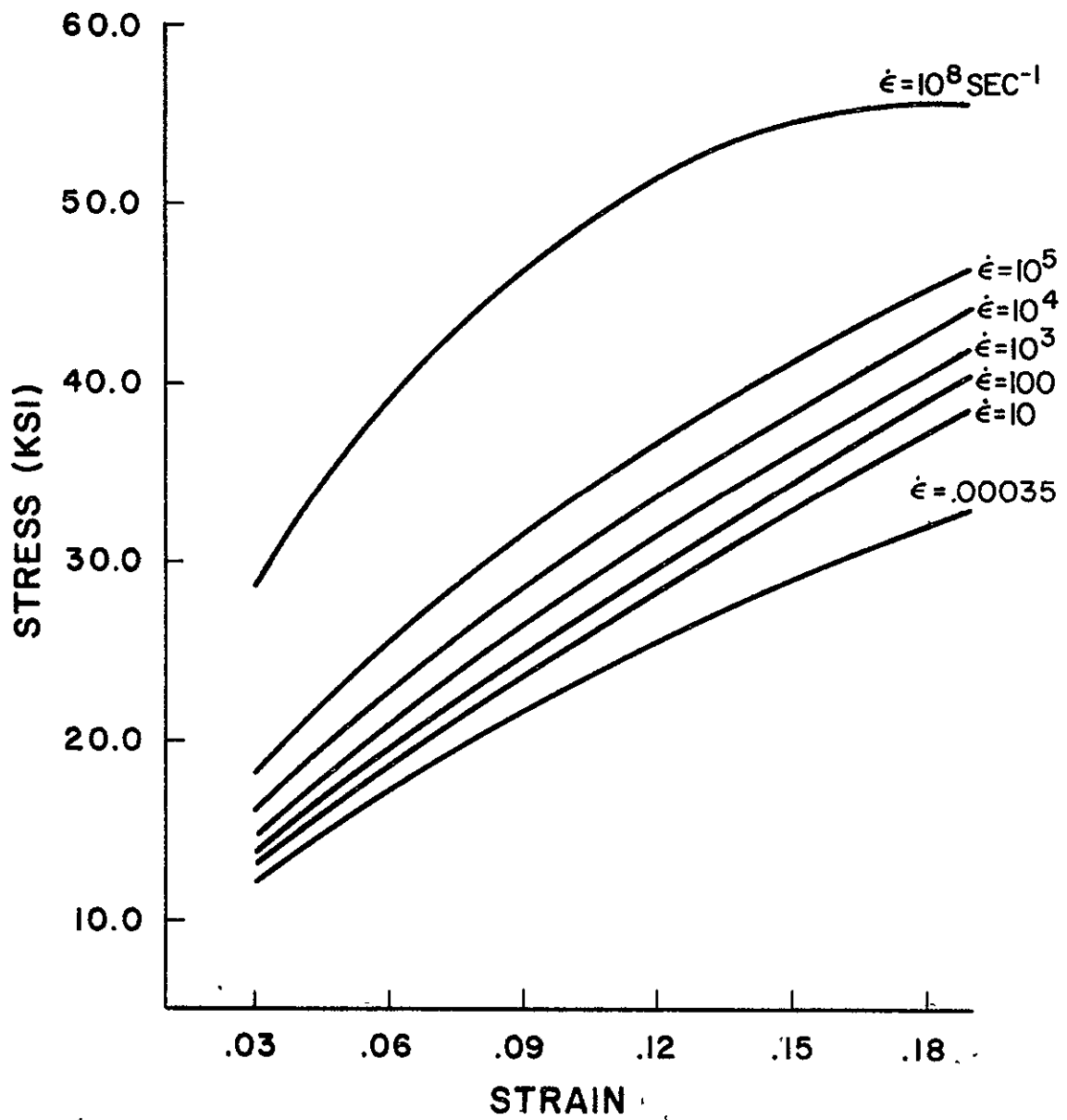


FIGURE II - DYNAMIC RESPONSE OF COPPER

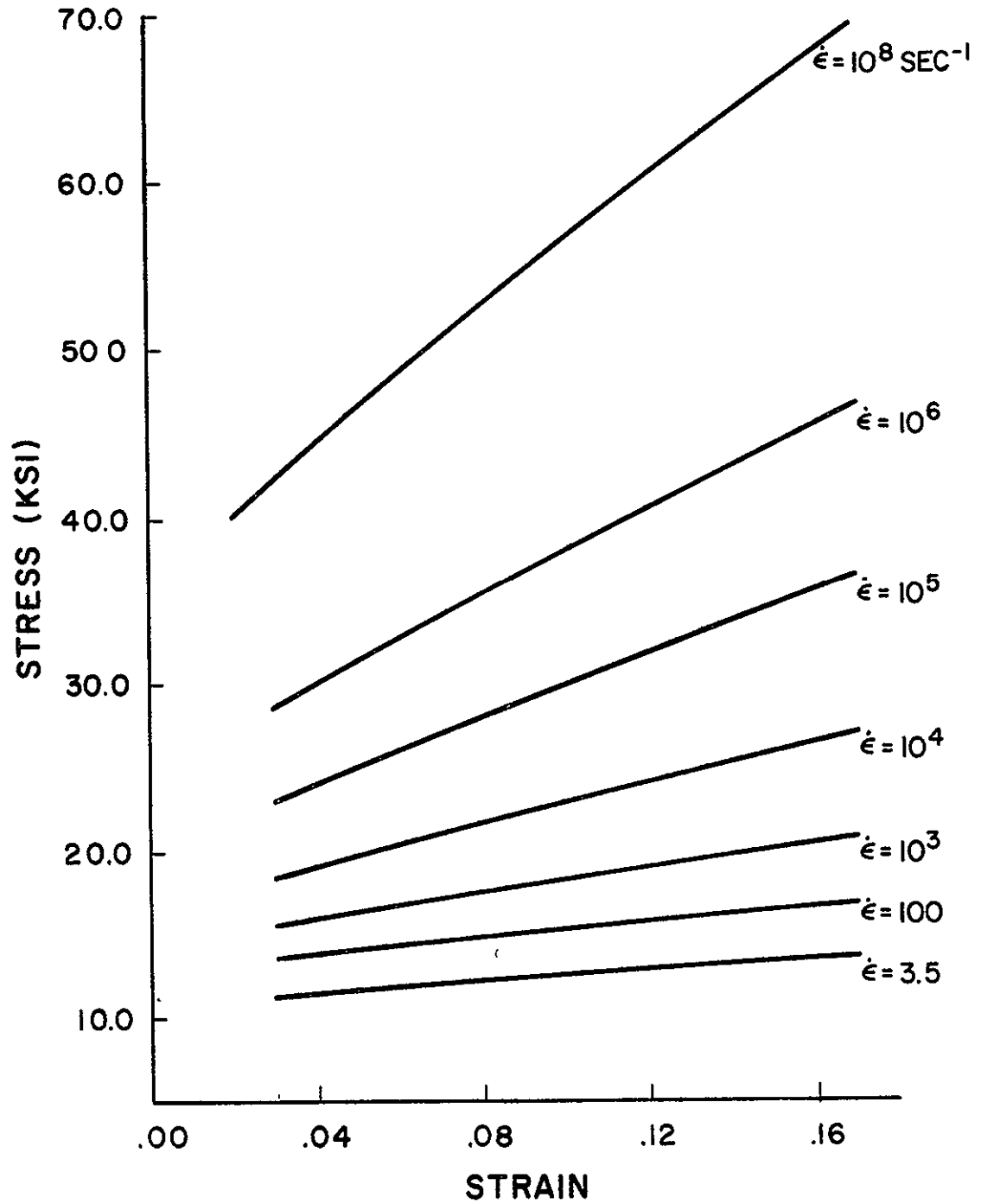


FIGURE 12 - DYNAMIC RESPONSE OF HIGH PURITY AL (99.997% PURE)

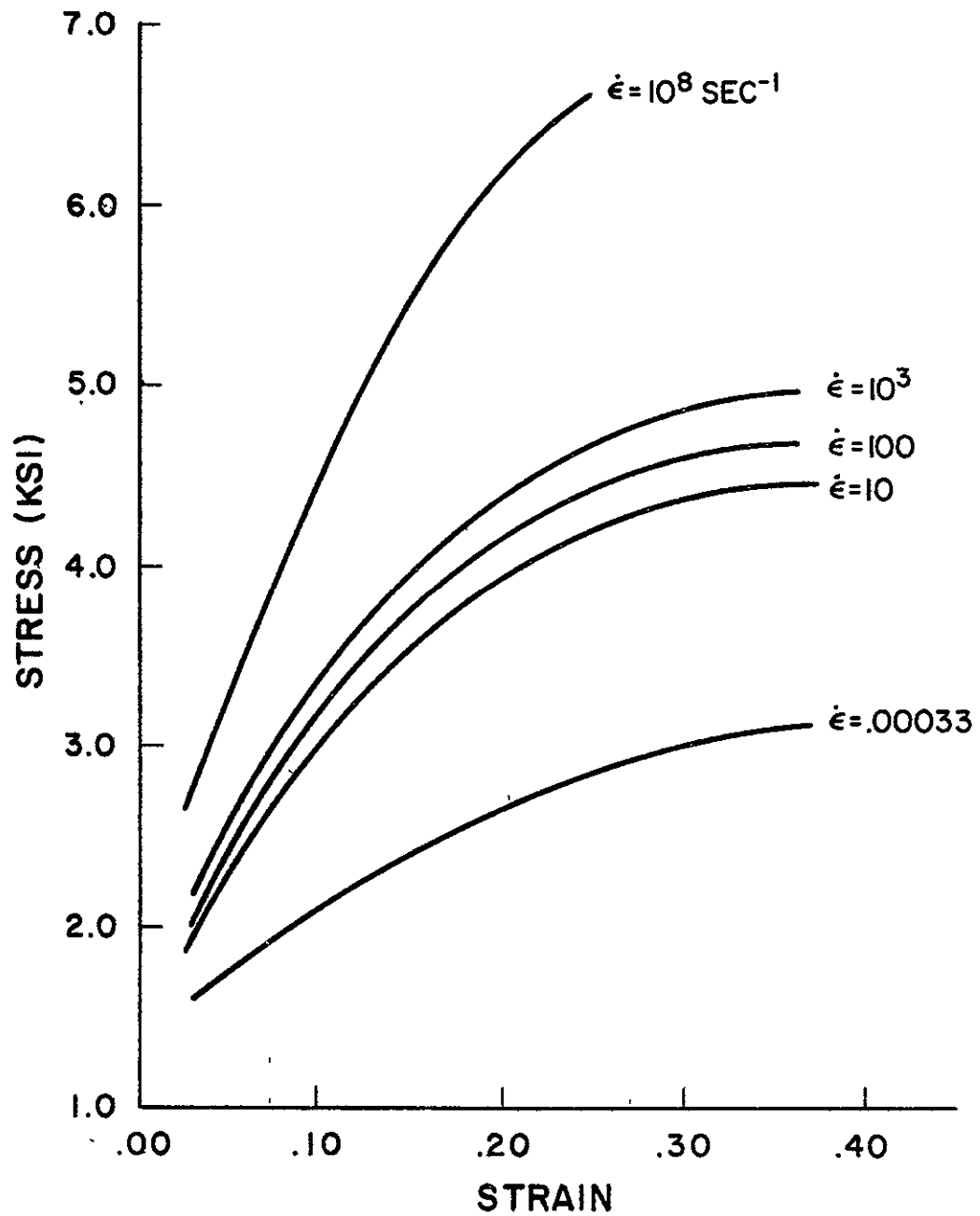


FIGURE 13 — DYNAMIC RESPONSE OF LEAD

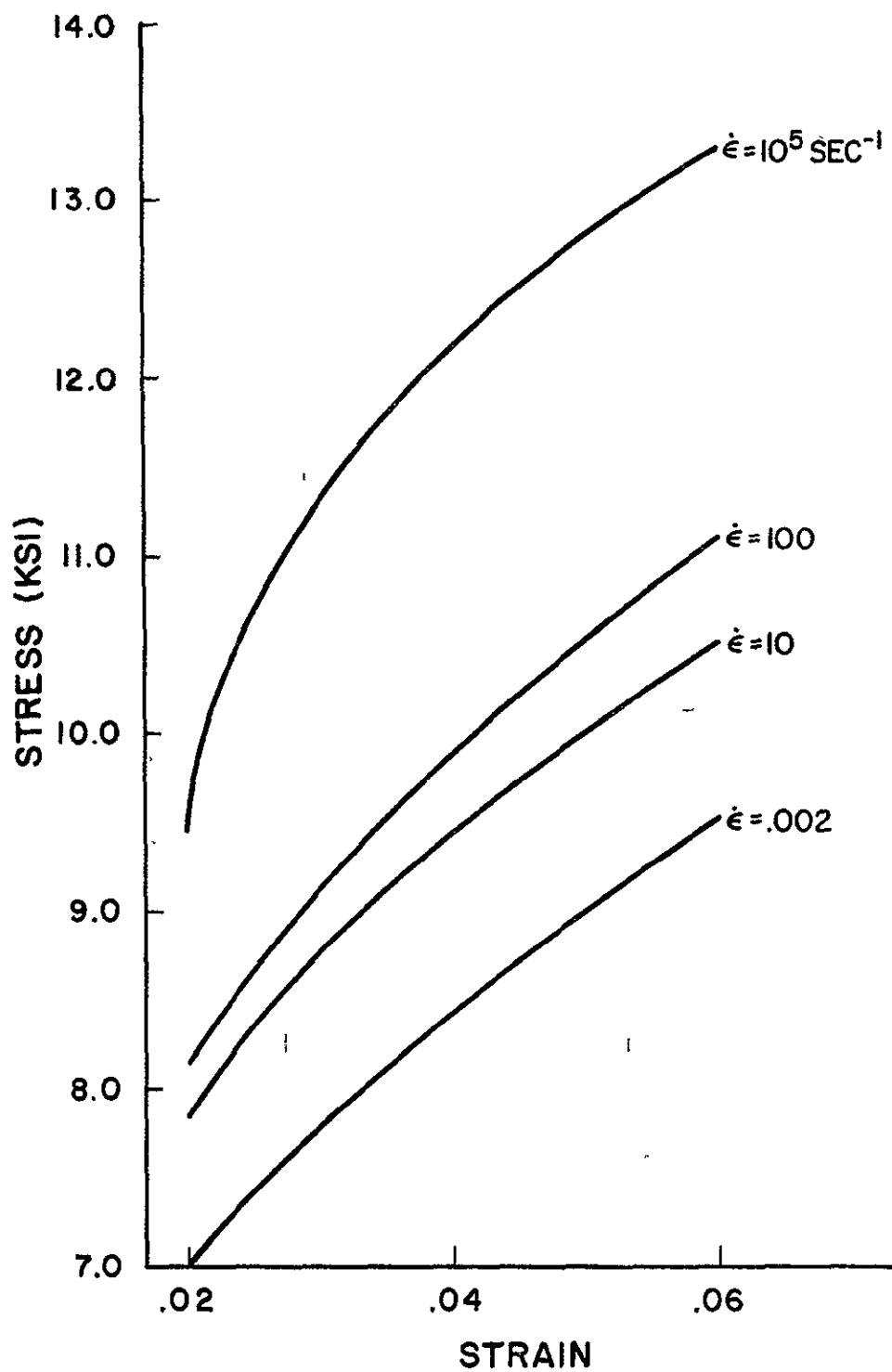


FIGURE 14 - DYNAMIC RESPONSE OF  
ALUMINUM 1060-O

## VITA

Charles E. Nelson was born on [REDACTED] in [REDACTED]  
[REDACTED], the son of H. E. Nelson and Mary E. Nelson. After graduation from Bishop Gorman High School, Las Vegas, Nevada, he entered Texas A&M University in September 1965. In May 1970 he received a B.S. degree in Aerospace Engineering from Texas A&M University and entered graduate school in June 1970 at the same university.

In the course of obtaining his Master of Science degree, he was sponsored by a NASA Research Grant working in the area of Hypervelocity Impact Effects. Upon graduation, he plans on working as a structural engineer.

His permanent address is 1018 Norman Avenue, Las Vegas, Nevada.

The typist for this thesis was Mrs. Pat Nunley.